NTNU

Norwegian University of
Science and Technology

Analysis and Design Bjørnefjorden TLP Supported Suspension Bridge subjected to Large Ship Collisions and Extreme Environmental Loads

Analyse og dimensjonering Bjørnefjorden
TLP understøttede hengebro utsatt for støt
fra store skip og ekstreme miljøkrefter

Victor Romero Zamudio

Maritime Engineering
Submission date: June 2017
Supervisor: Jørgen Amdahl, IMT

Norwegian University of Science and Technology
Department of Marine Technology

NTNU – Trondheim
Norwegian University of
Science and Technology

Analysis and Design Bjørnefjorden TLP Supported Suspension Bridge subjected to Large Ship Collisions and Extreme Environmental Loads

Victor Romero Zamudio

June 2017

PROJECT / MASTER THESIS

Department of Marine Technology

Norwegian University of Science and Technology

Supervisor 1: Professor Jørgen Amdahl

Norwegian University of Science and Technology (NTNU)

Trondheim, Norway

Supervisor 2: Professor Jonas Ringsberg

Chalmers University of Technology

Göteborg, Sweden

NTNU
Norges teknisk-naturvitenskapelige universitet
Institutt for marin teknikk

MASTER THESIS 2017

for

Stud. Techn. Victor Romero Zamudio

Analysis and Design Bjørnefjorden TLP Supported Suspension Bridge subjected to Large Ship Collisions and Extreme Environmental Loads

Analyse og dimensjonering Bjørnefjorden TLP understøttede hengebro utsatt for støt fra store skip og ekstreme miljøkrefter

The Norwegian Public Roads Administration (NPRA) is running a project "Ferry free coastal route E39", where the where suspension bridges, floating bridges or submerged tunnels would be installed across fjords in Western Norway. The straits are up 5 kilometres wide and will call for significant extension of present technology. Several innovative crossing concepts have been proposed. One of these is the TLP bridge concept, which consists of a 3-span suspension bridge, supported by two tension leg moored floaters and two fixed traditional concrete Pylons. The 3 main spans of the bridge have a length of 1385m. The side span on the south is approximately 300m and 353m at the northern end. The water depth is 550m at one floater and 450m at the other. The sketch below illustrates the technical concept of the Bridge

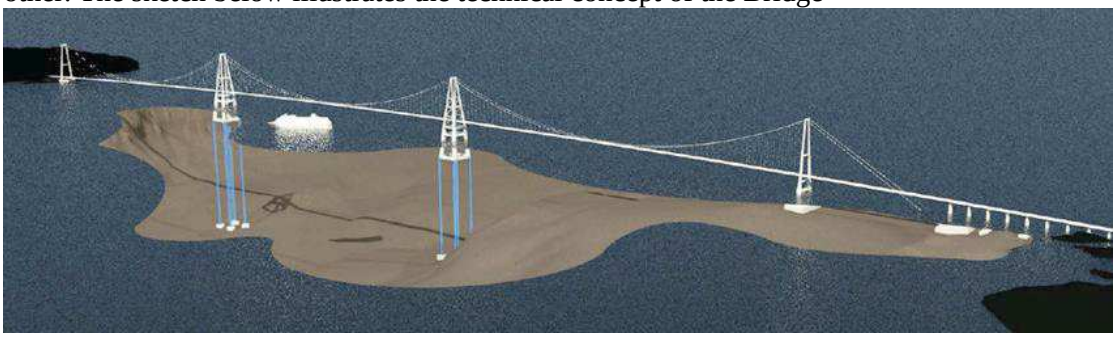

The bridge has to resist extreme environmental loads and accidental actions with acceptable safety levels. One of the concerns are accidental ship collisions with energies in the range of 100-1500 MJ. The proposed concepts cannot be designed adequately using existing methods and design rules. Consequently, advanced scenario-based analyses have to be conducted based on accurate simulation of the governing physical processes.

This TLP will be single leg floater with arms below the free surface for attachment of the tension legs. A floating ring structure at the free surface, which is connected to the tension leg attachment points and shall ensure sufficient stability in transport and installation phase,: It has been proposed that it should also be used as a device to absorb energy during a ship impact event. The ring will be pushed forward and due to this motion be submerged. The increased buoyancy and hydrodynamic drag should dissipate the major part of the collision energy.

The purpose of the work is to perform further studies on the bridges subjected to extreme environmental loads and ship collisions.

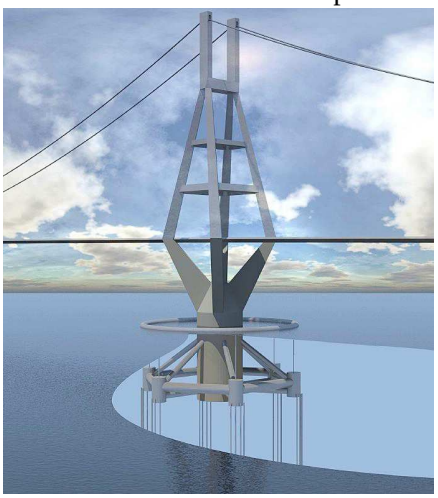

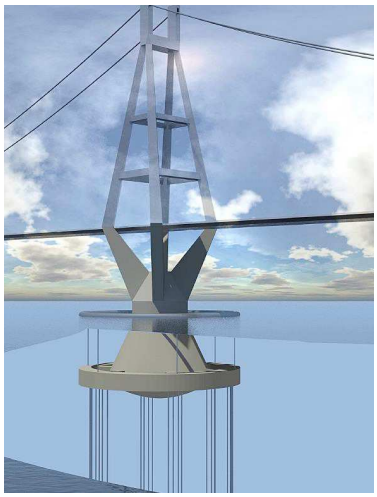

.

Scope of work:

1. Local design of the steel pylon against ship impact. Establish a model of the pylon in the water plane area for analysis with LS-DYNA. Conduct ship collision analysis for the bow of a container vessel and an ice-strengthened ro-ro vessel. Propose a pylon design that is highly resistant against ship collision.

2. Conduct dynamic, time domain simulation of ship collision with the bridge using USFOS. Updated ship force-deformation curve obtained from LS_DYNA analysis shall be modelled using the nonlinear spring concept. The ship shall be represented by a nodal mass with initial velocity. Central collisions shall be assumed initially.

3. Perform analysis of non-central impacts, where ship may be deflected away from the pylon. Use a new model for global ship motions provided that the model becomes available during thesis period.

4. Conduct residual strength analysis of the bridge with collisions damage exposed to extreme environmental loads. The effect of flooding of compartments caused by ship collision shall be included.

5. Simulate failure in the form of fracture of one or more tethers and estimate its effect on the stress/force levels in critical components. Explain the results. Let the fracture time vary. Conduct residual strength analysis of the bridge exposed to extreme environmental loads

6. Conduct analysis of the bridge subjected to extreme environmental loads using the contour line method applied to offshore structures. Analysis shall be carried out with both static and

stochastic wind loads, the latter using the WINDSIM software. Include relevant wave loads. Slowly varying drift forces and sum frequency forces shall be considered.

7. Conclusions and recommendations for further work

Literature studies of specific topics relevant to the thesis work may be included.

The work scope may prove to be larger than initially anticipated. Subject to approval from the supervisor, topics may be deleted from the list above or reduced in extent.

In the thesis the candidate shall present his personal contribution to the resolution of problems within the scope of the thesis work.

Theories and conclusions should be based on mathematical derivations and/or logic reasoning identifying the various steps in the deduction.

The candidate should utilise the existing possibilities for obtaining relevant literature.

The thesis should be organised in a rational manner to give a clear exposition of results, assessments, and conclusions. The text should be brief and to the point, with a clear language. Telegraphic language should be avoided.

The thesis shall contain the following elements: A text defining the scope, preface, list of contents, summary, main body of thesis, conclusions with recommendations for further work, list of symbols and acronyms, references and (optional) appendices. All figures, tables and equations shall be numerated.

The supervisor may require that the candidate, in an early stage of the work, presents a written plan for the completion of the work. The plan should include a budget for the use of computer and laboratory resources, which will be charged to the department. Overruns shall be reported to the supervisor.

The original contribution of the candidate and material taken from other sources shall be clearly defined. Work from other sources shall be properly referenced using an acknowledged referencing system.

The report shall be submitted in two copies:
- Signed by the candidate
- The text defining the scope included
- In bound volume(s)
- Drawings and/or computer prints which cannot be bound should be organised in a separate folder.

Supervisor NTNU:
Prof. Jørgen Amdahl

Deadline:, January 15, 2017

Trondheim, June 11 2017

Jørgen Amdahl

Preface

This master thesis is submitted to the Norwegian University of Science and Technology (NTNU) in order o fulfill the final requirement to obtain the Master degree in Maritime Engineering.

This thesis was developed under the supervision of Professor Jørgen Amdahl from the Norwegian University of Science and Technology as main supervisor and Professor Jonas Ringsberg as co-supervisor as part of the Nordic Master in Maritime Engineering.

The developed analytic work and the simulations for this master thesis were performed in the Department of Marine Technology of the Norwegian University of Science and Technology (NTNU), moreover the facilities and the required specialized software were provided by NTNU.

This masters thesis is aimed at readers interested in marine engineering, especially those interested in offshore structures, more specifically in floating bridges, collision simulations and simulation of the structural behavior of floating structures under extreme and accidental loading conditions. Although not mandatory, the present work considers that the readers have a technical background to make use of this material, therefore it is written in technical language.

Trondheim, 2017-06-11

Victor Romero Zamudio

Acknowledgment

First of all, I would like to thank Professor Jørgen Amdahl as my main supervisor to develop this thesis, at the same time to the Department of Maritime Technology of the Norwegian University of Science and Technology (NTNU). I am very grateful for the constant feedback to develop this thesis, for his recommendations and the experience shared by my supervisor. Professor Amdahl has been a constant motivation to conclude the work related to this project.

I would also like to thank Professor Jonas Ringsberg for his comments and feedback for this thesis. As my professor at Chalmers, he was an inspiration to continue my specialization on maritime structures.

I must thank my two educational institutions, the Norwegian University of Science and Technology and Chalmers University of Technology for giving me the opportunity to participate as a student, to every member of the Nordic Master in Maritime Engineering staff.

I would also like to thank Postdoctoral fellow Yanyan Sha for his continued advice and guidance throughout this project in order to conclude in time and accuracy.

Finally I would like to thank Norway and Sweden for being part of my education and personal growth. For all the amazing experiences which I will remember to participate in the creation of more equal societies.

Victor Romero Zamudio

Summary

The local analysis and structural design of the floating pylon for the Bjørnefjorden TLP Supported Suspension Bridge was performed. Ship collision analysis were conducted for the bow of a container vessel in order to design a pylon that is highly resistant against ship collision.

A preliminary design of the structural arrangement, the geometry and the mechanical properties of the pylon were proposed considering the general configuration. Later a finite element model considering the initial design was built in Patran software and refined in LS-DYNA software to simulate ship collision.

Collision simulations were conducted by using LS-DYNA in order to investigate the structural response of the pylon. The damage for both the vessel and the pylon were identified for different collision directions. The failure mechanism was investigated in relation to the force-deformation relation.

The structural performance of the pylon was studied in terms of the number of damaged compartments, the damage level, stress and strain levels, internal energy, pressures and the force-deformation curves.

The dynamic response of the bridge was investigated by carrying out time domain simulations using USFOS software considering accidental loads due to ship collision. To do so, the updated force-deformation curves from LS-DYNA were implemented for computations in USFOS. Collision simulations were conducted by using non linear springs to simulate the collision effect.

Residual strength analysis for the bridge were conducted considering flooded compartments. Moreover the dynamic response was studied in terms of the maximum displacements. Finally the failure in the form of fracture of one tether is included in order to study the variation of forces in critical components.

Contents

Chapter 1

Introduction

There is a current ongoing discussion related to how to promote the construction of infrastructure across Norway in order to communicate the country. According to Gudmestad (2013), when taking into account a commercial point of view, a communication link without ferries represent and advantage and the construction of bridges and tunnels to facilitate communication could reduce in travel time from 20 hours to 13 hours.

To do so, the Norwegian Public Roads Administration (NPRA) is running a project "Ferry free coastal route E39", in which suspension bridges, floating bridges or submerged tunnels would be installed across fjords in Western Norway depending on specific characteristics and requirements. At the same time NPRA studies the feasibility to replace ferry crossing of the 8 widest fjords on the west coast of Norway by fixed links Jakobsen (2013).

Due to the nature of the project, the current regulations might be a bit limited in terms of the specific characteristics of the bridge; furthermore, in order to estimate the response, detailed structural models must be studied using specialized software.

Skorpa (2013) considers that most important the E39 project faces considerable challenges. The Coastal Highway Route E39 are beyond any other bridge structure built today. Furthermore this is the first bridge project which meet the challenges regarding geometry, environmental conditions and ship traffic. As a consequence, the E39 project requires to overtake the existing engineering limits to develop new technologies in order to connect across the fjords.

Because of the extreme nature of this project in relation to daily ship traffic and possible accidental scenarios in which the bridge will operate, detailed structural models must be devel-

oped in order to analyze the structural response under accidental and extreme environmental loads. This scenario is where this thesis project finds its application as a study of the so called Bjørnefjorden TLP Supported Suspension Bridge.

1.1 Background

Seven of the most extreme fjords on the western coast of Norway are crossed by the Coastal Highway Route E39 from Kristiansand to Trondheim. Ferries currently cross the fjords; however the NPRA is planning to replace the ferry connections with fixed links Skorpa (2013).

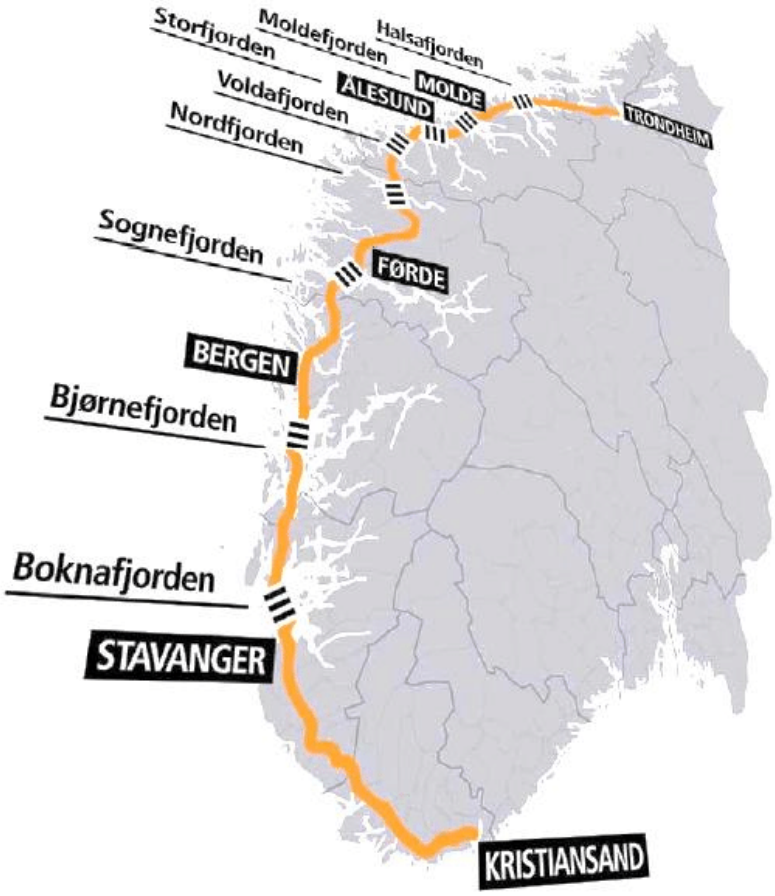

Figure 1.1: Coastal Highway Route E39, Mr. Olav Ellevset, (2014)

According to Statens Sta, the E39 project includes the design and construction of eight ferry crossing which are considered to be replaced by straights in which five are considered extreme cases requiring engineering innovations. Moreover the fjords have a width varying from 2 to 8

km and depths varying from 300 to 1300 m. Besides the topographic and bathymetric conditions, the bridges are required to allow free passage for cruise liners visiting the fjords Skorpa (2013).

The Symposiums on Strait Crossings will remained considered as an important topic until straits, fjords and sounds represent restrictions to road and rail transport. This means, there will be a continuous demand on creating more efficient, economic and environmental friendly solutions to cross straits, Erik Frydenlund, Kaare Flaate, Håvard Østlid (2005).

Improved mobility and the connections along Norway might be reached by constructing advanced infrastructure such as tunnels and bridges to cross the fjords and to reduce the transportation time. Advanced mathematical models are necessary to be developed. This project deals with the so called Bjørnefjorden TLP Supported Suspension Bridge which is analyzed and design considering accidental loads due to ship collision scenarios.

1.1.1 Extreme straight crossings, today's status

According to Statens vegvesen, the National Transport Plan (NTP) for 2014-2023 verified Parliament ambition to construct the "ferry free E39" a main connection road running from Kristiansand in the south of Norway to Trondheim in north. The stretch is about 1100 km long. Overall the project would pass through six counties and other visited cities such as Stavanger, Bergen, Ålesund and Molde.

Every year, the fjords are visited by cruise ships; furthermore the ship traffic should not be restricted by any fixed connection. Besides this initial challenges, other aspects must be taken into account such as life cycles costs and energy considerations. According to the Japan National Tourism Organization(JNTO) there are several existing examples of developments related to fjord crossings, some in Norway and some abroad. A first example is the Akashio Kaykio suspension bridge in Japan which is considered the world's largest suspension bridge linking Awaji Island and Kobe. The total span is about 3911 m. It is also considered the tallest structure in Japan with two towers of 300 m above the sea level, JNT.

Figure 1.2: Akashi Kaikyo Bridge, Aka

One of the floating bridges in Norway s the so called Nordhordland Bridge which is a combination of cable a stayed bridge, a pontoon bridge and a viaduct connecting both sides in Hordaland Norway. The total length is about 1914 m and a height equal to 99 m, the clearance is 32 m which allows for a sailing channel, Nor (b).

Figure 1.3: Nordhordland Bridge, Nor (a)

The last bridges are two example of the current state of art. Developing the technology to design and construct the structures for the CHRE39 must be supported by the marine knowledge, the Norwegian experience in the offshore industry and bridge engineering. There are several experiences related to bridge design; however as mentioned before the structures contemplated by this project are beyond any other existing structure.

1.1.2 The Bjørnafjorden TLP Suspension Bridge

The Bjørnefjorden TLP Supported Suspension Bridge has particular characteristics which make it unique in its type. This bridge consist of a 3-span suspension bridge with floating supporters including tension legs and two concrete pylons, the Bjørnefjorden project considers an approximated length of 1385 m for the three main spans.

At the same time, the side spans consider 300 m for the south side and 353 for the north side. Besides the last structural elements, the considerable depths of the fjord reach about 550 m at one of the floaters and 450 m for the other. Fig. 6.1 shows the lateral drawing provided by the supervision.

Lidvard Skorpa reports that close to the deepest part of the sea bead, soft sediments are found; furthermore, the gained experience from the offshore industry may be applied to the anchoring system. Close to the shallow part, the seabed is solid rock, Skorpa (2013). Due to the specific characteristics of Bjørnafjorden, different possible solutions might be design, from submerged tunnels to floating bridges might be feasible; however for the approach of this thesis, the solution is base on tension leg platform (TLP) technology.

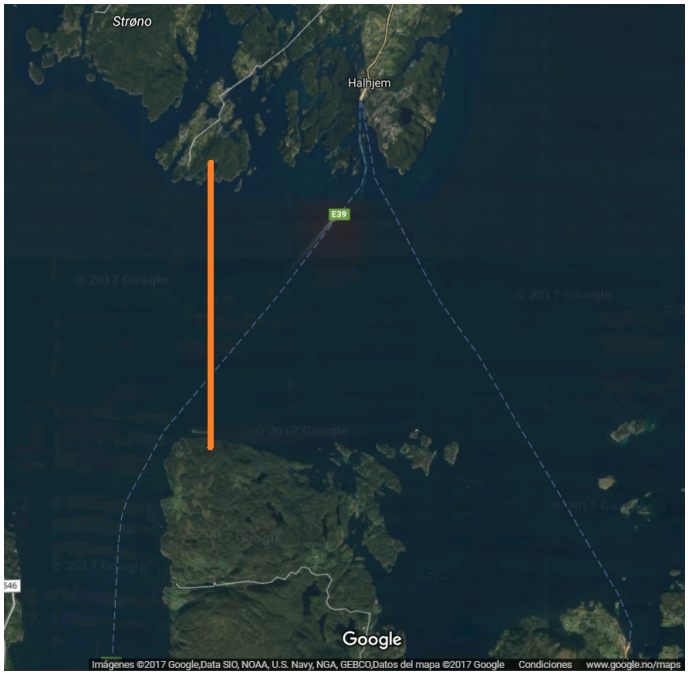

Figure 1.4: Location Bjørnafjorden bridge, Norway, Goo

1.1.3 Objective

The objective of this thesis is to analyze the structural behavior of the floating pylon of the bridge, considering possible ship collision scenarios in order to design a structure highly resistant to collision.

To achieve this, a finite element model of the pylon was constructed by using specialized software in finite element method in order to conduct collision simulations. A main objective was to design the global structural configuration and the detailed structural elements conforming the pylon by an iterative procedure. Finally, it is sought to study the global dynamic response of the bridge under this collision scenario, as well as the effects on the residual strength considering the effects of flooded compartments of the pylon and a possible case of fracture of tethers.

1.1.4 Thesis distribution

This thesis is organized in chapters, which are ordered with the intention of presenting the developed work in the clearest way. A brief summary of the chapters is presented below:

- Chapter 1 presents a brief introduction to the problem under study, the state of the art, the motivation and a review of the background to this project.
- Chapter 2 introduces the necessary theory used in relation to the principles of structural modeling, ship collision and regulations on accidental loads.
- Chapter 3 presents the modeling procedure to achieve the pylon model. The suggested geometry, the mechanical characteristics and the boundary conditions. A brief introduction of the ship model is included as well.
- Chapter 4 focuses on the LS-DYNA Finite Element Model, the geometry description, material properties, the meshing process and the collision.
- Chapter 5 introduces the most important results from LS-DYNA.
- Chapter 6 contains the collision simulations using USFOS, a brief description of the structural model and the results of the dynamic response of the bridge under accidental loads.

- Chapter 7 presents the results of a bridge residual resistance analysis considering the effect of collision damage, flooding of compartment, failure in the form of fracture of tethers and its effects on stress/force levels.

- Chapter 8 discusses the modelling assumptions, the complexities in the process and general results.

- Finally chapter 9 presents the main conclusions and recommendations for future work.

1.1.5 Scope and limitations

The scope of this thesis project has been limited to those suggested by Professor Amdahl in the project description, in which the particular scope is described in detail.

The work scope proved to be larger than initially anticipated, thus the project was reduced in extend by not performing the analysis related to environmental loads in USFOS. From an overall perspective, the time was considered a limitations for this project because the model construction in LS-DYNA followed a long iterative schedule.

Subsequently the simulations in LS-DYNA and the optimization and redesign processes took a considerable time, later the USFOS simulations and the subsequent analyzes have been developed in approximately one month. Under this scenario, this document is strongly focused on the collision analysis conducted in LS-DYNA and the collision simulations in USFOS.

Chapter 2

Theory

This chapter introduces the necessary theory throughout this project. A brief description on the principles of structural modeling and analysis is introduced. In addition, it includes the analysis of ship collision and some of the current regulations.

2.1 Principles of structural modelling using FEM

The finite element method (FEM) is a numerical approach used to solve several problems in science and engineering. The general approach is to solve partial differential equations by using numerical computations to approximate the solutions. From an overall perspective, there are several FEM applications in engineering, for example, stress analysis, heat transfer, electromagnetic, fluid flow, among others Jacob Fish (2007).

For this thesis, a finite element model was constructed to analyze the structural behavior of the bridge pylon. On the other hand, if the reader is interested in the mathematical formulation which is the theoretical base of the FEM model, it is recommended to consult specialized literature.

Diverse references are feasible to be consulted but a first recommendation is the LS-DYNA theory manual John O. Hallquist (2006) which contains the main theory considered by this software with a extensive discussion on the governing equations and deep theory on beam and shell elements. FEM models have numerous applications which are developed with academical, industrial, researching purposes, among others. So specific references might suit better for

specific applications.

To estimate the behavior of structural and mechanical systems in relation to design and performance, the whole system is divided in finite elements connected by nodes. In order to reach a continuous system, the nodes must be shared by implementing a continuous mesh.

To obtain more accurate solutions when using FEM, a mesh with a large number of elements is usually required, later the mesh is used to solve partial differential equations by mean of computational calculations. Usually the precision of the approximation improves with a greater number of elements; however the main disadvantage is the cost of computation time, since it increases with the number of elements.

There is a long history of development of the finite element method followed by the parallel development of specialized software for its application. Institutions such as NASA have funded projects to develop finite element programs, such as NASTRAN developed in California with a group of professionals led by Dick MacNeal with diverse applications in applied mechanics Jacob Fish (2007).

Another example of these software is LS-DYNA developed by Livermore National (LLNL) Laboratory, this software finds its main applications in dynamic nonlinear analysis, impact analysis, analysis of fall, among others.

To develop this thesis, the structural model was first constructed using Patran, which uses the principles of the NASTRAN code and later used LS-DYNA to perform the nonlinear dynamic collision analysis.

2.2 A brief introduction about LS-DYNA software

LS-DYNA was developed in the mid seventies and the first version was introduces in 1976 for solid elements with 4 or 8 nodes considering constant stress. Several improvements were implemented for the following versions, by refining more efficient algorithms. Later new features were implemented such as additional materials and vectorization of velocities. The software capabilities were improved for every new released version and many extensions and capabilities had considerable progress until reaching the last versions. Extensive improvements in the results were made by adding new control algorithms and boundary considerations.

According to LLNL, LS-DYNA is a code which finds its main purpose in analyzing large deformations under static and dynamic load cases by applying explicit time integration methodologies. The most recent version includes adapting meshing and a variety of element formulations such as: solid elements, two node beam elements, three and four node shell elements, eight node shell elements and rigid bodies John O. Hallquist (2006).

2.3 Introduction to ship collision

According to Professor Jørgen Amdahl (2001), one of the major hazards for offshore structures is related to the possibility of collision with ships. To this end, this accidental loading scenario is considered by various design codes such as NORSOK. On the other hand, in the event of a collision, the involved kinetic energy is usually very high, and the design of fixed and jack up platforms to this scenario is limited by the nature of the collision.

There are several studies boosting the quality of the regulations in terms of ship collision in order to be implemented. At the same time, the classification societies such as Det Norske Veritas and Germanischer Lloyd (DNV-GL), the American Bureau of Shipping (ABS) among others consider the accidental loads as a mandatory scenario for design.

To investigate the accidental limit state for ship collisions, nonlinear finite element techniques are used to obtain the response of the structures. These methodologies consider the use of finite element models of the ship and the particular installation under study and the way both interact with each other by assuming specific contact characteristics. The nature of the finite element analysis represents a challenge of modeling and computational analysis.

An accidental collision state may be described in terms of the kinetic energy involved. In such a case, when a collision scenario is presented, the kinetic energy is dissipated as deformation energy in both the structure and the ship. To this end, this condition involves considerable plastic deformations that can occur both the ship and the pylon.

The recommended Practice DNV-RP-204 deals with the design against accidental loads in order to maintain the load-bearing function of the structure during accidental events. As the recommendation specifies, the main objective of design against accidental loads is to accomplish a system which main safety functions are not degraded DNV-GL (2010). Ship collisions,

dropped objects, fire and explosions are covered by this document.

Of important relevance, the American Bureau of Shipping (2013) includes an analysis of accidental scenarios experienced by offshore and gas facilities which present during the installation, operation and decommissioning. Few extra cases considered by ABS are the blast hazard and the application of the regulations to the survival of permanent mooring systems under extreme environmental loads.

Remarkable definitions

There are several definition considered by the DNV-GL, some are taken from DNV-GL (2010) and described below as considered remarkable in relation to this thesis.

Accidental event: Considered as an undesired condition which might be combined with other conditions (e.g. failure of protection structures, environmental conditions, or extra combined loads) outline the accidental effects.

Accidental effect: Heat flux, motions, energy dissipation, impact force Consequences of the accidental event which is understood as a consequence of the accidental event.

Direct design: Judgment of the structural strength, material properties and dimensions in order to achieve a specific design and structural performance.

Acceptance criteria: Definition of the acceptable values of critical deformation, critical deflection or any critical response to avoid damage propagating to other structural elements, causing damage to the equipment or leakage of compartments.

2.3.1 Design philosophy

The design philosophy against accidental thinks of inhibiting any incident to magnify into a disproportionate accident from the original cause. The design may be done by direct impose of the effects on the structure. To do so, it is mandatory to apply experienced engineering judgment and pragmatic evaluations, DNV-GL (2010).

When analyzing ship collision, two main scenarios are required to be studied. First the structure must be looked over by applying the loads developed during the collision. And secondly when the structural capacity is reduced as a result of the accident, it is necessary to analyze the

structure under ordinary loads. Later, the structure must be assessed for the applicable limit states.

Eq. 2.1 introduces the general requirement of the accidental limit state according to DNV. For the ALS to be checked the load and material factor should be taken as 1.0.

$$Sd \leq Rd \tag{2.1}$$

where

$S_d = Sk\,\gamma_f$ Design load effect

$R_d = Sk\,/\,\gamma_M$

S_k = Characteristic load effect

γ_f = partial factor for loads

R = Characteristic resistance

γ_M = Material factor

2.3.2 Distribution of strain energy dissipation

Frequently the kinetic energy characterizes the ship collision, which is influenced by the mass and speed of the ship, including the added mass. Conditioned by the collision conditions, the kinetic energy might be dissipated as strain energy or remain as kinetic energy. Normally large plastic deformations present under collision scenarios, furthermore either the vessel, the facility or both present damaged DNV-GL (2010).

Under this consideration, it is understood that depending on the deformation energy that each system takes (the installations and the ship), we should find ourselves in one of the three zones of design, ductile design, shared energy design or strength design.

Fig. 2.1 introduces the energy dissipation for strength, ductile and shared-energy design.

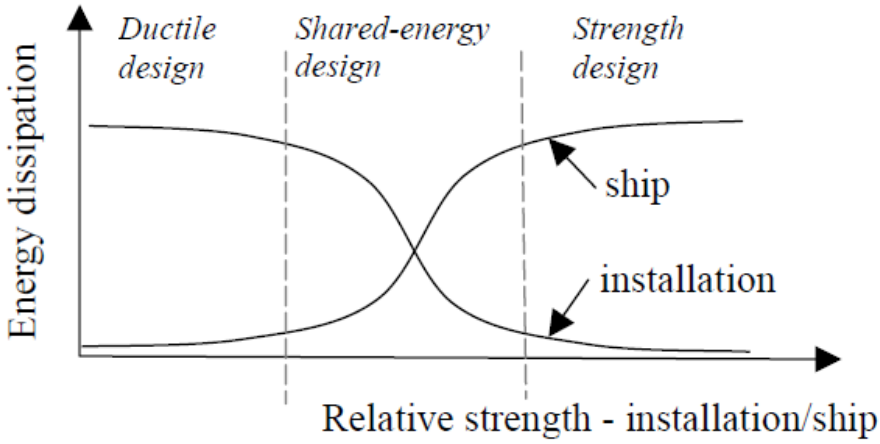

Figure 2.1: Energy dissipation for strength, ductile and shared-energy design DNV-GL (2010)

Under the ***strength design*** zone, the installation facilities are assumed to be strong to counteract the collision force with minimum deformations, the deformation energy is dissipated by large deformation of the ship; while the ***ductile design*** design zone considers the deformation energy is mostly taken by the structure, on the other hand when referring to the ***shared-energy*** zone, it is understood that both the ship and the installations will share the deformation energy.

To investigate ship collision, several cases may be contemplated, multiform studies have been conducted worldwide depending on the needs for every project. However, for this thesis the case of ship collision with large diameter columns is considered more representative, due to the specific dimensions of the structures.

The interacting structures are the ship and the pylon of the floating bridge. From this perspective, in the event of a collision, both structures will be damaged. However, the pylon of the bridge represents a fundamental structure for its safety and the failure of this represents the possibility of total collapse, besides the meaningful repairing costs.

On the other hand, the damage to the ship is no less important; however, depending on the collision and the characteristics, the structural damage of the ship might lead to a state of alert or loss of hydro static stability that motivates amplified dynamic responses. However, it is difficult to assess at first impression the collateral damage.

For this project, the damage of the pylon is tried to be reduced to a minimum so that greater deformation energy is dissipated by the ship. This assumptions takes us to achieve a design

under the strength design zone, which implies less possibilities of bridge collapse and reduction of repair costs.

2.3.3 Collision mechanism

DNV-GL suggests that when the duration of the impact is small compared to the fundamental natural period of the facility, the structure may be assumed as compliant, but when the duration of impact is larger than the fundamental natural period, the structure may be considered fixed DNV-GL (2010).

Harald O. (2016) reports the bridge has a fundamental natural period of 104.4 s and the collision is expected to blast few seconds. A value of 124.77 s was estimated by hand calculations by Romero V. (2016). Furthermore the Bjørnefjorden TLP supported suspension bridge subjected is considered compliant asshown in eq. 2.2.

$$\mathrm{E}_s = \frac{1}{2}(\mathrm{m}_s + \mathrm{a}_s)\mathrm{V}_s^2 \frac{(1-\frac{\mathrm{V}_i}{\mathrm{V}_s})^2}{1+\frac{\mathrm{m}_s+\mathrm{a}_s}{\mathrm{m}_i+\mathrm{a}_i}} \tag{2.2}$$

where

m_s = ship mass

a_s = ship added mass

v_s = impact speed

m_i = mass of installation

a_i = added mass of installation

v_i = velocity of installation

J = mass moment of inertia of installation (including added mass) with respect to effective pivot point

z = distance from pivot point to point of contact

2.3.4 Ship collision assessment

The American Bureau of Shipping (2013) separates the collision assessment in internal and external energy mechanisms. The rigid body motions of the ship are addressed by the external

mechanism while the structural failure of the bodies is accounted bythe internal energy. This approach may be summarized as below,

Accoring to ABS, ship collision energy balance may be expresses in terms of eq. 2.3,

$$E_{KE,init} = E_{ext} + E_{int} \tag{2.3}$$

The initial kinetic energy of the colliding vessel is decomposed by means of internal and external mechanisms as shown in eq. 2.4.

$$E_{KE,init} - (E_{KE,f} + E_{KE,v}) = (E_{SE,f} + E_{SE,v}) \tag{2.4}$$

where

$E_{KE,f}$ = facility kinetic energy after contact

$E_{KE,v}$ = colliding vessel kinetic energy after contact

$E_{SE,f}$ = facility strain energy

$E_{SE,v}$ = colliding vessel strain energy

A strain energy is developed as structural deformation, the energy balance can be expresses as curves in terms of the dissipation of strain energy. An idealized resulting scenario is shown in fig. 2.2, the relationship between an applied collision load (F) and the resulting information (u).

A rapid interpretation of this image is that the damage increases with increasing deformation. The damage might grow from the local buckling to the rupture of outer and inner shells. The same reasoning applies for the vessel and the facility.

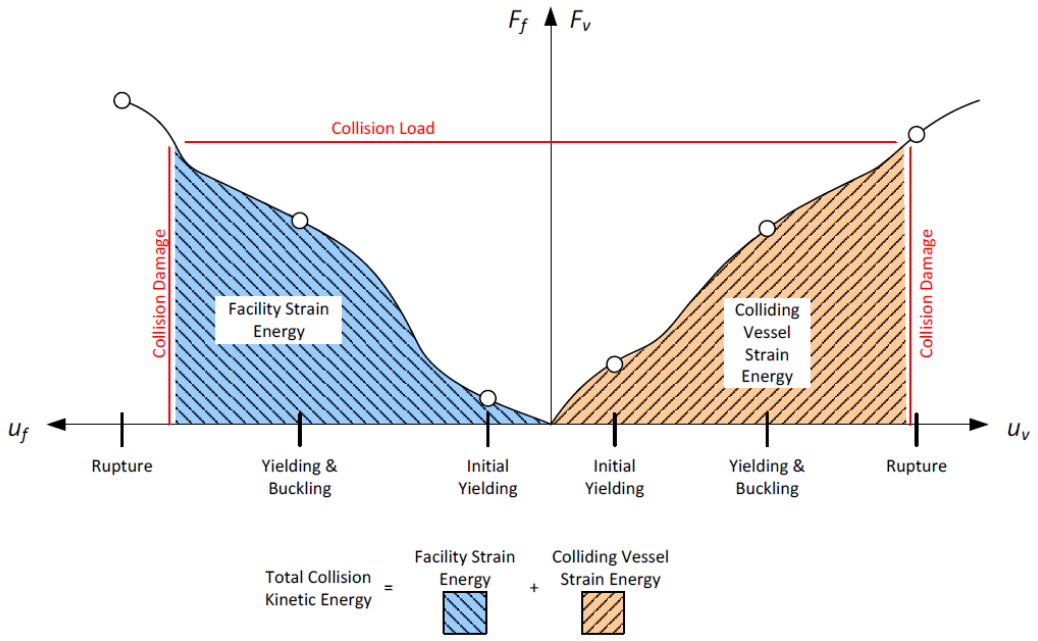

Figure 2.2: Dissipation of strain energy in ship and platform American Bureau of Shipping (2013)

From the American Bureau of Shipping (2013) regulations, fig. 2.3, three methods to determine the damage level in the ship and facilities.

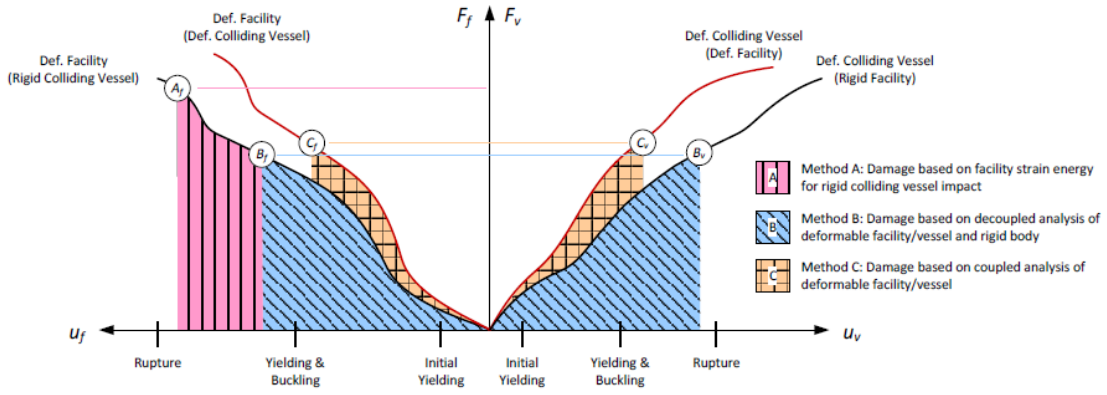

Figure 2.3: Dissipation of strain energy in ship and platform American Bureau of Shipping (2013)

Method A is the most conservative because it considers a rigid body colliding with the facility (A_f), then the kinetic energy is accounted by the facility deformation.

Method B is less conservative than method, two separated analysis are performed, one for a rigid vessel colliding a deformable facility (B_f) and one for a deformable vessel colliding a rigid facility (B_v).

Method C is considered as the least conservative because it considers the additional effect of impact force being distributed out and the strain energy developed in both bodies for the ship (C_f) and for the installation (C_v). Besides the last three methods, for estimating the strain energy of the last approaches, there are two general categories of methods feasible to use, static approximate finite element analysis and dynamic finite element analysis.

2.3.5 The force-deformation curve

To study the collision mechanism, a particular interesting result is the force-deformation relationship which is plotted in force-deformation curves. Different ships will interact differently with the facilities, this relationship depend on the structural characteristics of the vessel and the facilities. On the other hand, the interaction properties between both bodies have important influence on these results.

Recommended curves are given by the classification societies, fig. 2.4 shows one example from DNV.

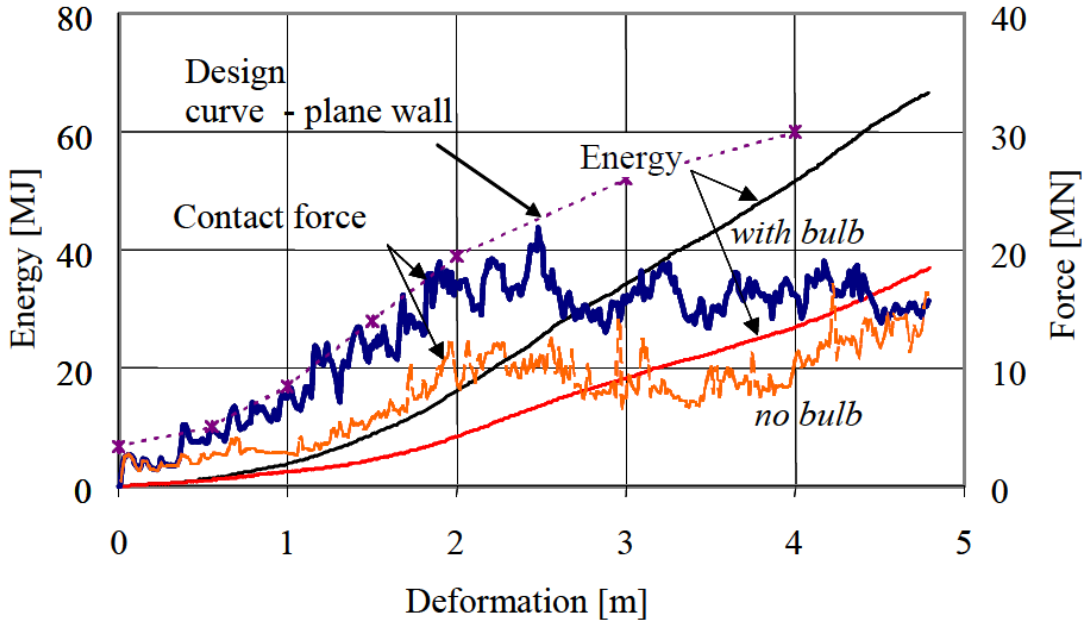

Figure 2.4: Force-deformation relationship for bow with and without bulb (2-5.000 dwt) DNV-GL (2010)

Chapter 3

Initial design of the steel pylon

This chapter describes the procedure followed for achieving an initial design of the bridge pylon, as a summary of the different stages along the model creation. At the same time, the global and detailed initial dimensions are introduced as well as the structural elements that built it up.

3.1 Design background

Several studies have been conducted in relation to ship collision simulations, this is the case of the impact analysis of submerged floating tunnels developed by Yun Lee (2013). The current state of art of the ship collision simulations in relation to strait crossing concept considers colliding ships with considerable dimensions and capacities with the floating pylons or submerged tunnels. Collision simulations using nonlinear finite element analysis against a multi-span bridge were performed by Yanyan Sha (2017).

For the Bjørnefjorden TLP Supported Suspension Bridge, previous studies have been conducted. This is the case of the master thesis developed by Harald O. (2016), who studied the dynamic response of the bridge considering a protecting ring surrounding the pylons.

This study considers a vessel colliding the pylons without any barrier and causing considerable damage to the structure. To investigate the structural response, a FEM model was built.

3.2 Model description

To accurately build a model, three main categories of information must be filled up, the geometry, the mechanical properties of the material and the load cases. These characteristics are described below.

3.2.1 General geometry description

Firstly, the general dimensions of the ship and the pylon are introduced. Fig. 3.1 sketches a top view of both bodies. The system considers a ship bow length of about 20.4 m and width equal to 26.4 for the largest cross section, while the pylon is a structure with circular cross section with a diameter of 30 m.

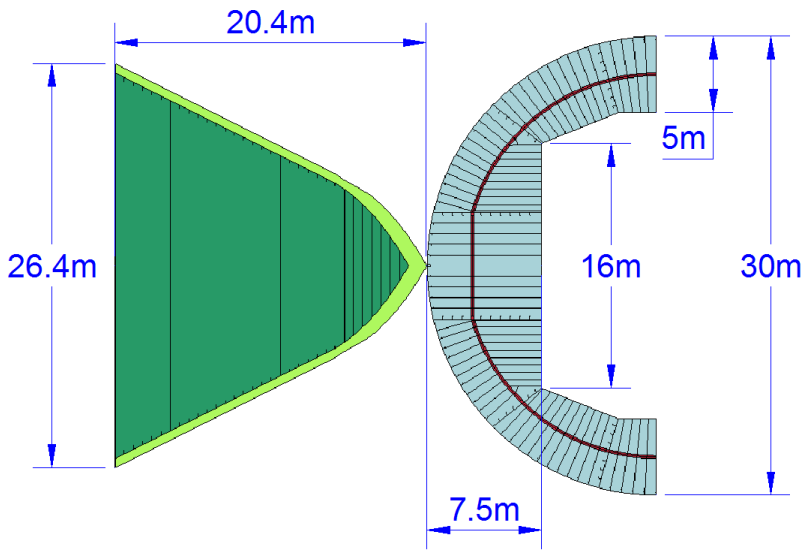

Figure 3.1: Top view of the ship and pylon

Based on this configuration, collision may present with several directions; therefore in order to identify structural damage accurately, it is advisable to investigate the effect of ship collisions with different orientations.

Fig. 3.2 sketches a lateral view, the total height of the pylon is about 33 m, the mean waterline is consider to be 0+000, while the bottom plate is located at -12+000 and the top plate is at 21+000.

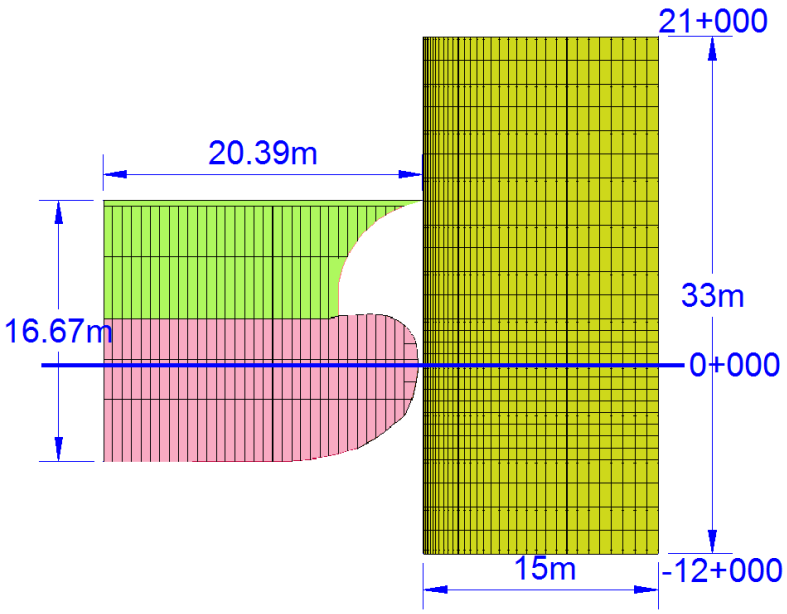

Figure 3.2: Sketch lateral view of the ship and pylon

The structure under the pylon is not considered for the simulations because the ship would not contact the substructure and considering it would increase the computation time.

3.2.2 Collision scenarios

When assessing accidental loading mechanisms, a traditional hazard identification method must be involved. The potential for accidental loading is examined in relation to the hazards, the risk exposure and the estimation of consequences. The likelihood is estimated for particular scenarios in order to support the design by providing sufficient structural stiffness, American Bureau of Shipping (2013).

The potential accidents are studied by the scenario hazard evaluation by using two main approaches, the hazard control and the predictive hazard evaluation. The last addresses the hazards that might not be considered by the hazard control approach.

Under real circumstances, the last studies are mandatory; however for this project, there was no scenario hazard evaluation for the identification of collision scenarios; however, it was proposed to vary the collision direction in order to identify the worst case of damage.

For this study three scenarios were considered, collisions with directions of 0°, 45° and 90°

were investigated as shown in fig. 3.3.

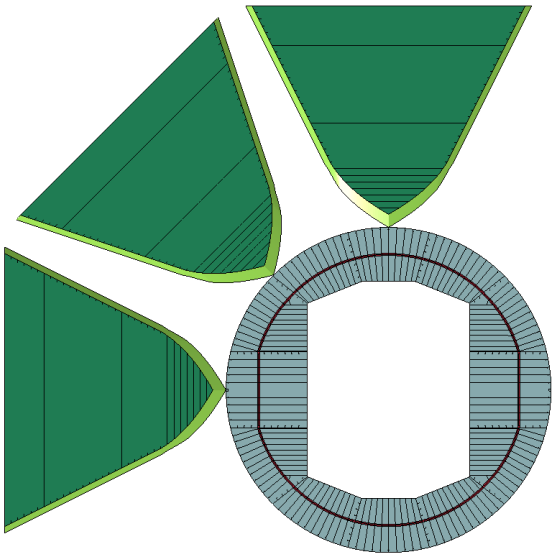

Figure 3.3: Possible collision directions.

The main reason for assuming different collision directions is to identify the most vulnerable areas of the structure. Although many other directions can be considered, this analysis was limited to the three previously mentioned. This analysis allowed to identify the damages generated with different angles of collision.

3.3 Ship description

For the offshore industry, when assessing ship collision, different operational regions consider notable differences in mass for supply vessels. For example vessel mass of 8,000 and 2,500 tons are considered for the North sea while 1,000 tons are considered for the Gulf of Mexico by the American Bureau of Shipping (2013).

However the ship a container ship is used for this analysis, furthermore the mass is far from the last range.

3.3.1 Detailed geometry description

For later simulations, a ship model constructed in LS-DYNA was provided by Professor Amdahl J. and Yanyan Sha.

The ship bow used for this study is based on a container ship of 20000 DWT. The ship considers an overall length of 166.62 m, with a module breadth of 27.4 m, a the depth of 13.2 m and a scantling draught of 9.6 m.

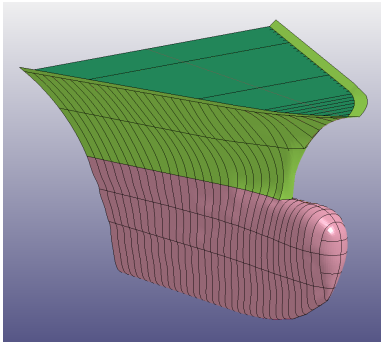

Figure 3.4: Isometric view

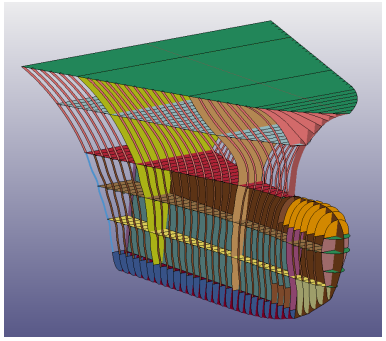

Figure 3.5: Internal structure

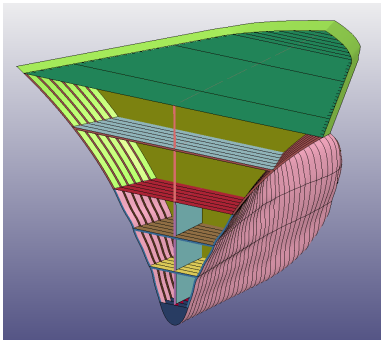

Figure 3.6: Back view

The various decks, stringers, transverse frames are modelled in addition to the shell panels. The vertical stiffeners have a spacing of 0.6 m. Only the first 20 meters of the ship bow are model for this study.

3.3.2 Materials

To perform initial simulations, the same steel was assigned to the ship and the pylon. The density, young's modulus, Poisson's ratio, shear modulus, bulk modulus, yield stress are shown in table.3.1. Steel S275 has been used as an equivalent to ASTM A36. These properties were modified later along the design process.

Table 3.1: Displacements, accelerations and forces under the collision simulation.

Steel properties for Steel S275								
γ	E	ν	G	B	σ_y	K	n	eps
kg/m3	Pa	–	Pa	Pa	Pa	Pa	–	–
8750	2.1E11	0.3	7.96E10	1.73E11	2.75E8	8E8	0.161	0.005

3.4 Modelling procedure

A structural model of the pylon was built to conduct ship collision simulations using LS- DYNA. To do so, the procedure was completed by following different stages. This section describes the followed procedure to reach a representative model.

3.4.1 Model creation

The creation of the model contemplated three main stages, first bi-dimensional proposals of the pylon were drawn, different structural configurations were made in AutoCAD with the intention of having a pre-design. As a second step, the geometry nodes were imported into the Patran software, in which the geometry was defined and the mesh was built up. Finally, before any computation, the third stage consisted of a refinement of the model using LS-Prepost. The above steps are described in more detail bellow.

Previous information

Information about the pylon and the flotation system was provided as images Jørgen Amdahl (2017). In order to built the model, this information was read visually and interpreted to reach a more detailed configuration. Fig. 3.7 presents a top and isometric views of the pylon and the floating structure.

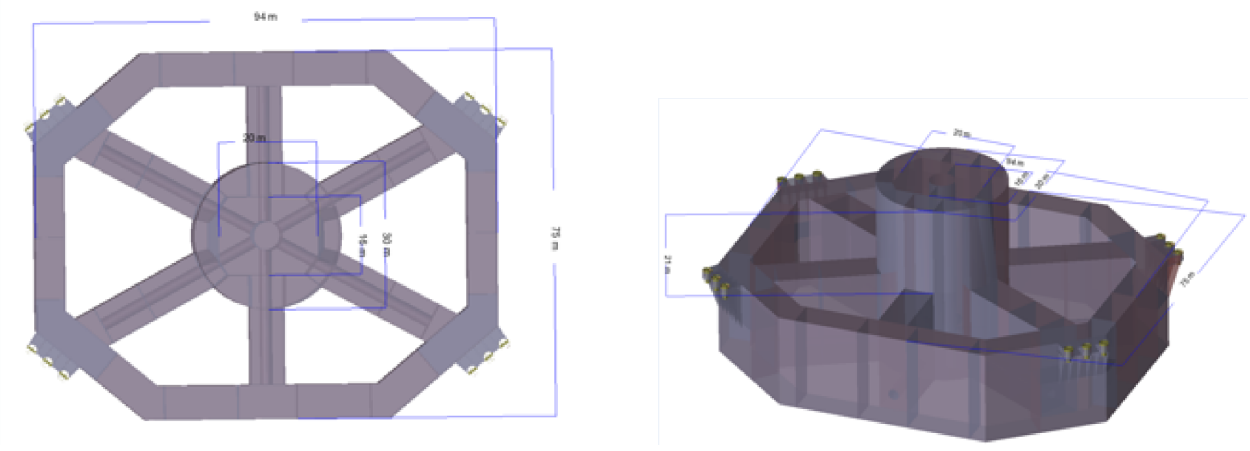

Figure 3.7: Top and isometric view of the pylon and pontoon.

A detailed isometric view is provided in fig. 3.8. Based on this figure, a vertical structural configuration was identified accordingly to dimensional approximations and visualized number of stiffeners.

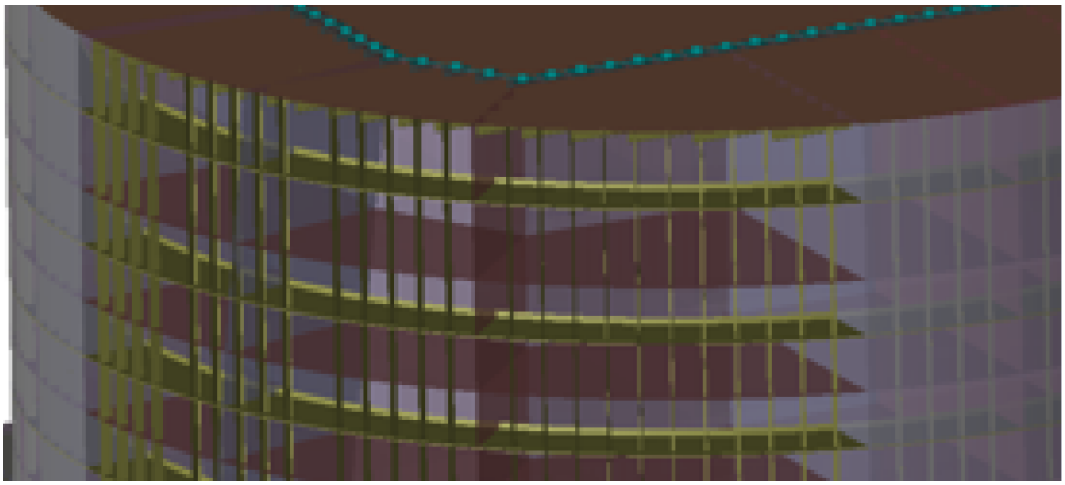

Figure 3.8: Isometric view of the pylon structure.

The decks separations was defined as 3 m with stiffening rings in between (1.5 m above every deck). The vertical stiffeners considered an approximated separation between 680-700 mm, based on the supervisor's experience.

Initial propose in Autocad

As in any structural design, the first step required a pre-design. Based on the experience of Professor Amdahl J., pre-dimensions were proposed for the thicknesses of the flanges and webs for stiffeners and girders. At the same time, the dimensions of the deck and perimeter plates were based on externally suggestions.

Fig. 3.9 presents a pre-design for the stiffeners arrangement, the number of stiffeners is included for every compartment.

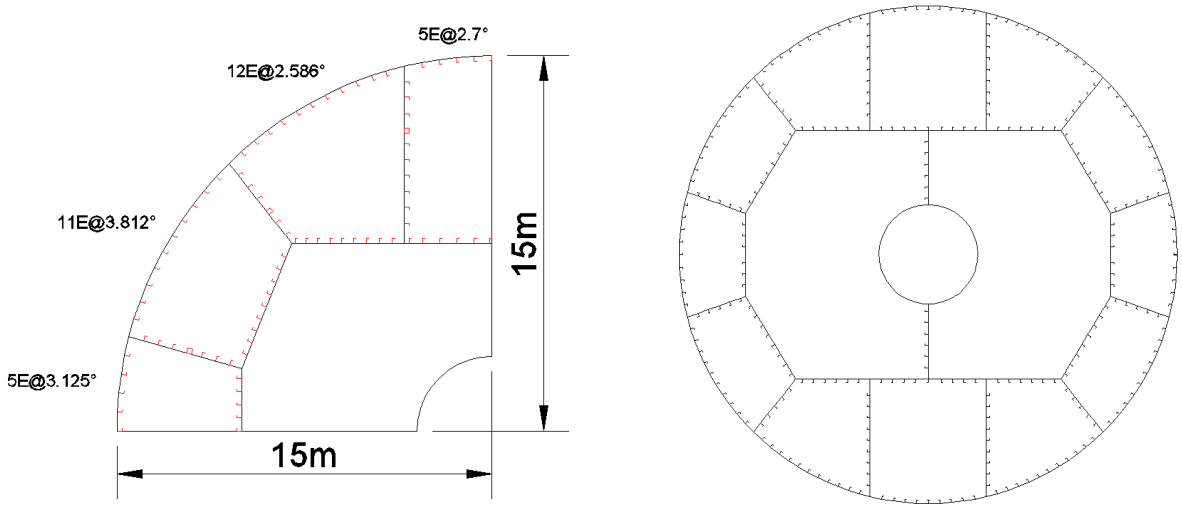

Figure 3.9: Pre-design of the stiffeners arrangement

In parallel, several configurations for the beam girders were proposed in order to achieve continuous frame work. The geometry and structural arrangement was proposed by taking into account the future design of the mesh for the finite element model. Therefore, the geometry considered the necessary aspects to achieve a continuous mesh as well. Fig. 3.10 shows the final arrangement of the girders. Annex 2 includes some extra arrangements which were considered limited either for achieving efficient frame work or inefficient mesh.

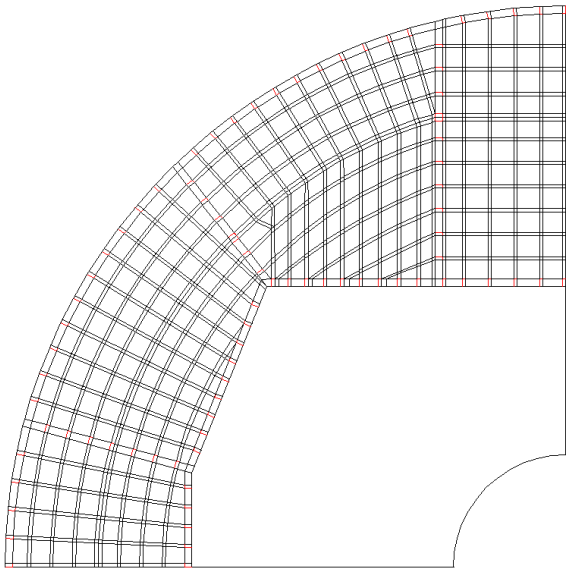

Figure 3.10: Structural arrangement for the girders

It is observed in the figure that the structural arrangement follows a radial configuration in order to achieve the continuous frame work. The radial girders are supported by a radial stringer. This stringer has been proposed to reinforce the work of three-dimensional frames and decrease the total length of the beams.

Modelling using Patran

Once the pre-design was proposed, the next step consisted in constructing the structural model of the pylon in Patran software. The modeling procedure is summarized in the following steps:
1.- Import of the pre-design nodes in file .out to Patran.
2.- Connection of the nodes.
3.- Creation of the plates based on lines and the imported nodes considering the continuity of the plates.
4.- Creation of structural groups for the parametric design in later stages.
5.- Matching the structural frames.
6.- Definition and assignment of material properties (Elastic phase).
7.- Assignment of thicknesses by groups of structural elements.
8.- Verification of the mesh continuity by means of detailed inspection.

A top view of the model in Patran is shown in fig. 3.11. It might be seen that the structural arrangement corresponds to the pre-design.

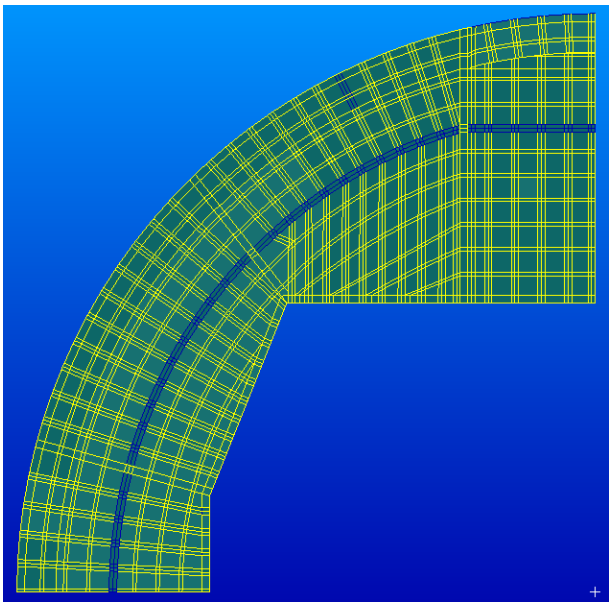

Figure 3.11: Top view - Patran model

It should be noted that the pattern made in patran corresponds to only a quarter of the cross section of the pylon. A height of only 1.5 m height was modeled, this height corresponds to the existing between the lower deck and the stiffening ring.

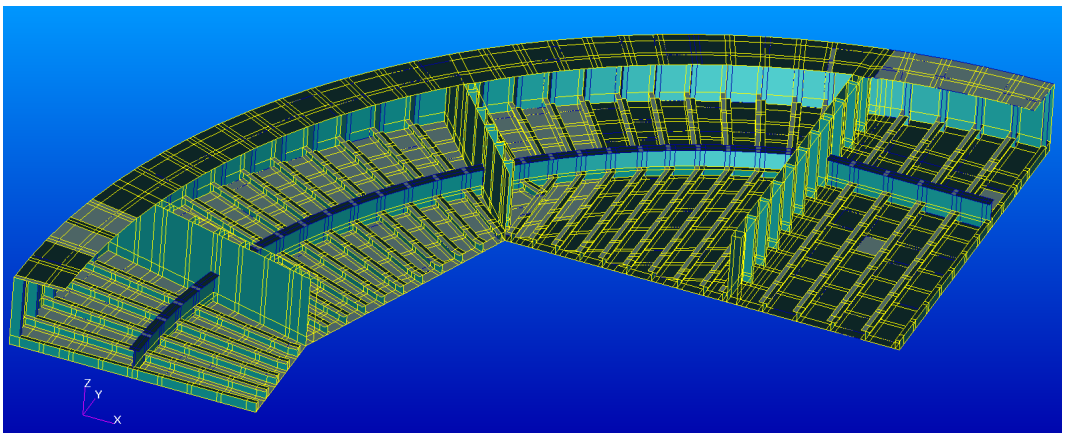

Figure 3.12: Isometric view - Patran model

Modelling using LS-PrePost

When the geometry mesh was finished in Patran, the next stage consisted of refining the model and assigning the boundary and contact conditions in LS-PrePost. The refining process of the

model consisted of:

1.- Refinement of the elements with inconvenient geometry for the computation.

2.- Repetition of the model to construct the complete pylon.

3.- Identification and elimination of duplicate nodes.

4.- Assignment of plastic properties to the models.

5.- Definition of the self body contact conditions for both structures.

6.- Definition of surface-to-surface contact conditions.

The elements of the finite element model that make up the structure are described in more detail below. A top view using LS-PrePost is included in fig. 3.13.

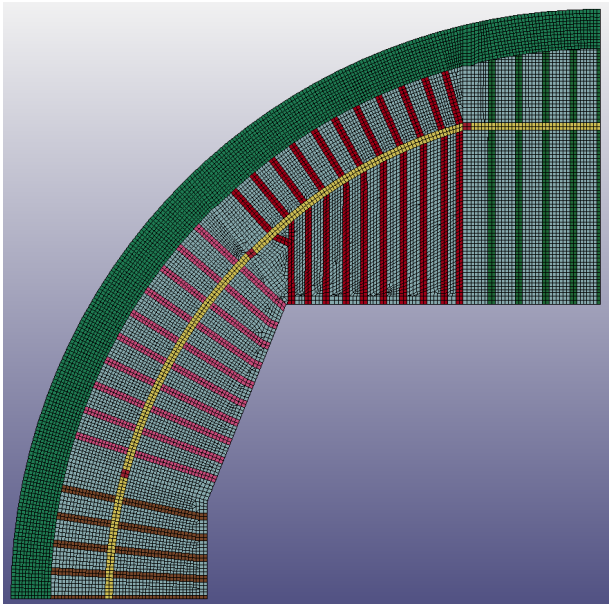

Figure 3.13: Top view - LS-DYNA model

Fig. 3.14 introduces an isometric view of the model.

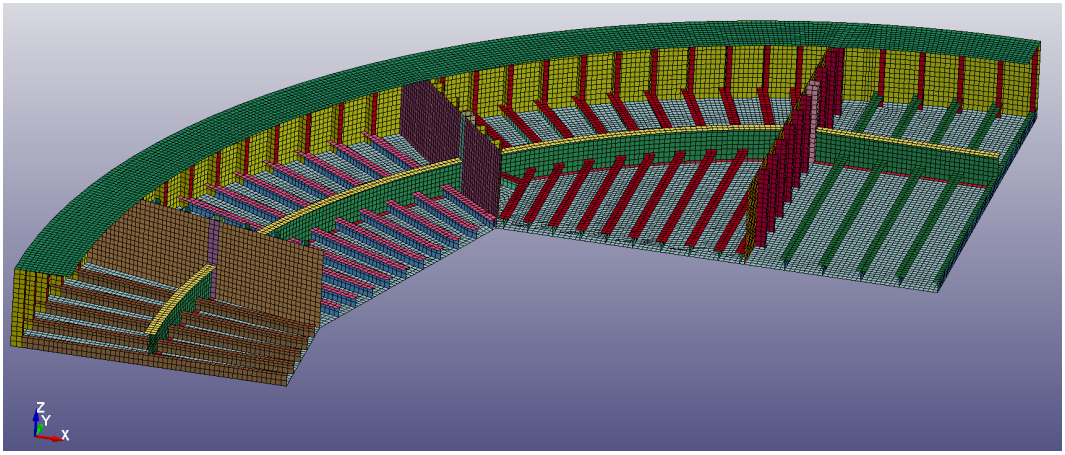

Figure 3.14: Isometric view - LS-DYNA model

So far, only one deck has been constructed because by ensuring continuity of a deck, it can be repeated later to achieve the configuration of the entire structure. This was done later in LS-PrePost to construct the complete model.

Collision simulations using LS-DYNA

Once the model was improved and refined in LS-PrePost, it was possible to conduct simulations in LS-DYNA. To do this, initial tests were performed with LS-Manager from a personal computer to verify the continuity of the the model. In the initial tests, new errors were identified and corrected by an iterative process. In the next chapter, the model constructed in LS-PrePost is discussed in more detail. Later on, the simulations were ran by using Vilje SGI Altix ICE X system, cluster provided by NTNU.

Chapter 4

Finite Element Model using LS-DYNA

This chapter presents the process to achieve a representative model in LS-DYNA.

4.1 Introduction to LS-DYNA

According to Livermore Software Technology Corporation LSD, "LS-DYNA is a general-purpose finite element program capable of simulating complex real world problems", there are several applications in different industries such as, the automobile, aerospace, construction, military, manufacturing, and bioengineering.

There are several softwares that might be suitable to use in order to pre and post-process the LS-DYNA model, this is the case of the software used along this thesis, the so called LS-PrePost, which is distributed freely and does not need a license.

Full 2D and 3D simulations, nonlinear and rigid body dynamics, quasi static simulations, linear statics, thermal analysis, fluids analysis, FEM-rigid body dynamics, failure analysis are some of the LS-DYNA's analysis capabilities, among others, LSD.

4.2 Elements description and mesh creation

The structural elements are presented to identified the main arrangements defined to built up the pylon.

Bottom and top deck panels

The model of the decks is shown in fig. 4.1. Such decks are formed by 4 structural panels, the plates have a thickness equal to 14 mm, separated by bulkheads. A radial stringer (I610X158) was proposed to reinforce continuous frame work. The girders (T203x37.3) were positioned with a radial orientation to reduce the lengths. The vertical separation between decks is 3 m.

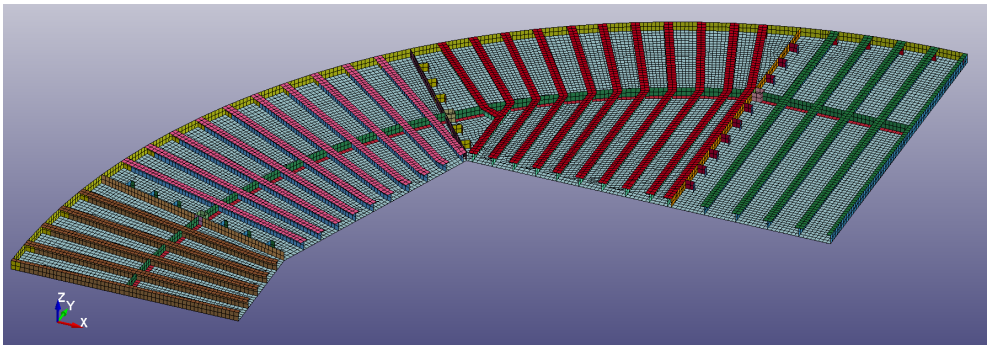

Figure 4.1: Configuration of the top and bottom decks

Stiffening ring

There is one stiffening ring between the decks in order to increase the strength of the structure. The width is proposed to be 1 m and the thickness is 14 mm.

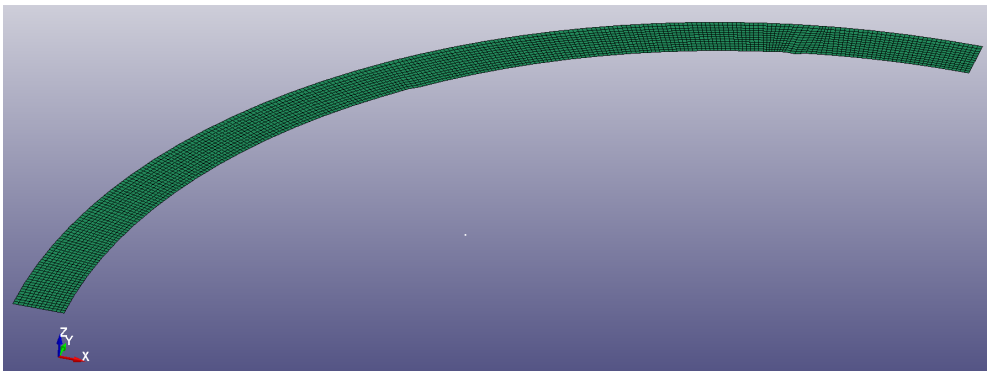

Figure 4.2: Stiffening ring

Internal bulkheads

To build the internal compartments, three vertical bulkheads are reinforced with stiffeners (L200X90). At the same time, a column (HSS203x9.5) is proposed to support the radial stringer. The same

configuration is used for the whole height. The configuration of the bulkheads are shown in fig. 4.3.

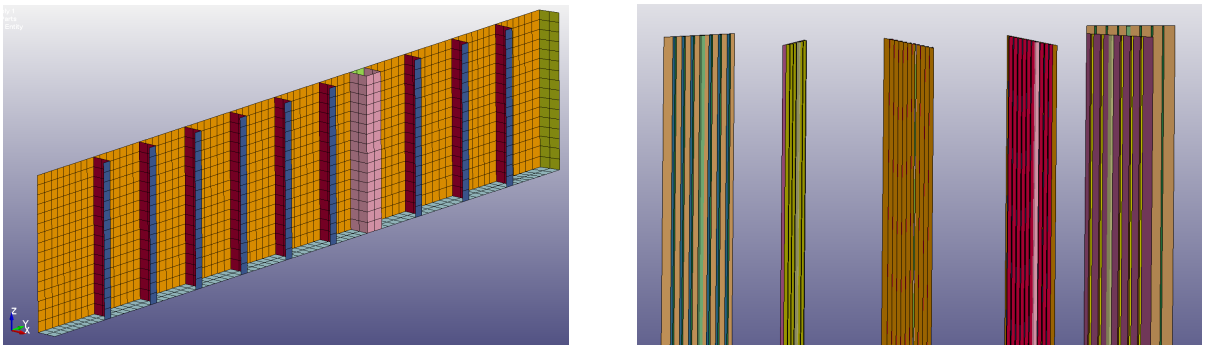

Figure 4.3: Bulckheads configuration

Perimeter panel and outer plate

One of the most important structural systems is the perimeter panel because this is the first structure to contact the vessel during the collision. The correct design of the perimeter panel will allow a more efficient distribution of stresses in the event of a collision. A closeup view is shown in fig. 4.4, the stiffeners (L200X90) are positioned vertically along the whole height and the plate thickness is 16 mm.

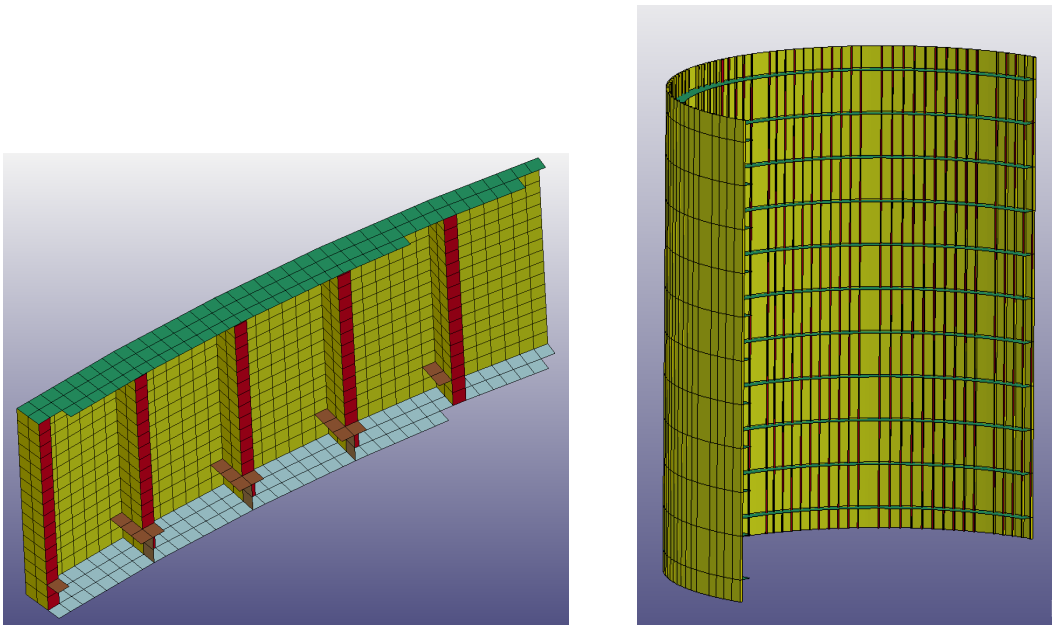

Figure 4.4: Perimeter panel

4.2.1 Mesh creation

As previously mentioned, to ensure accuracy in finite element analysis results, it was necessary to achieve the continuity of the mesh. The details of the mesh and the connection between the previously described elements are shown below. Fig. 4.5 exemplifies a convergence points where the deck, girder, and stiffeners are connected.

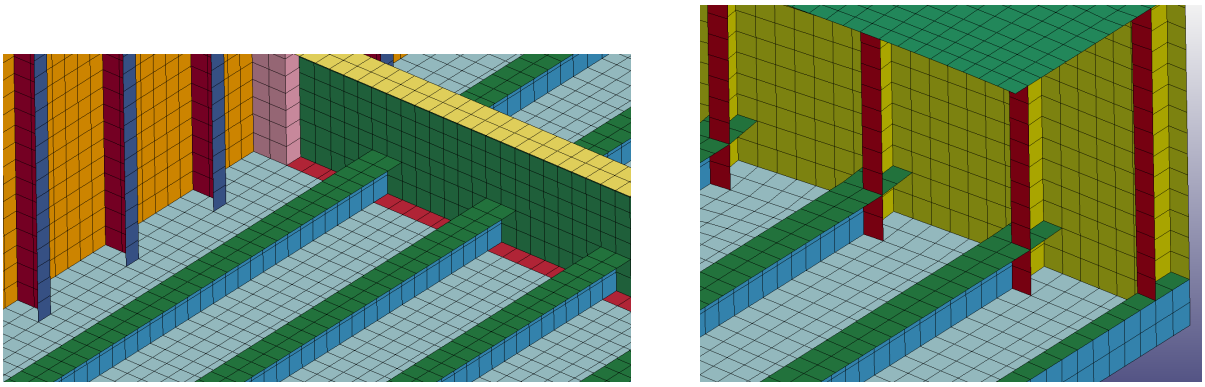

Figure 4.5: Continuity of the mesh

The meshing procedure was long and repetitive because the creation was done by a trial and error procedure, so the geometry and the mesh was done repeatedly until the continuity of the model was achieved.

Structural arrangement

Guaranteeing continuous frame work of the model is highly important. The final configuration achieved global and mesh continuity.

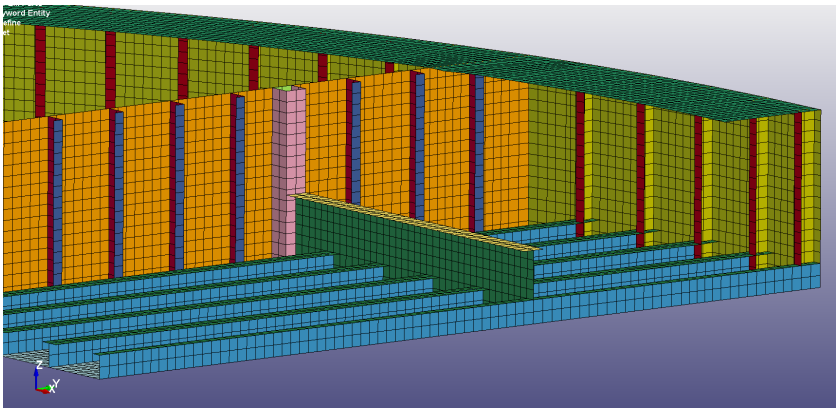

Figure 4.6: Close up of the structural configuration

The whole structure is displayed in fig. 4.7.

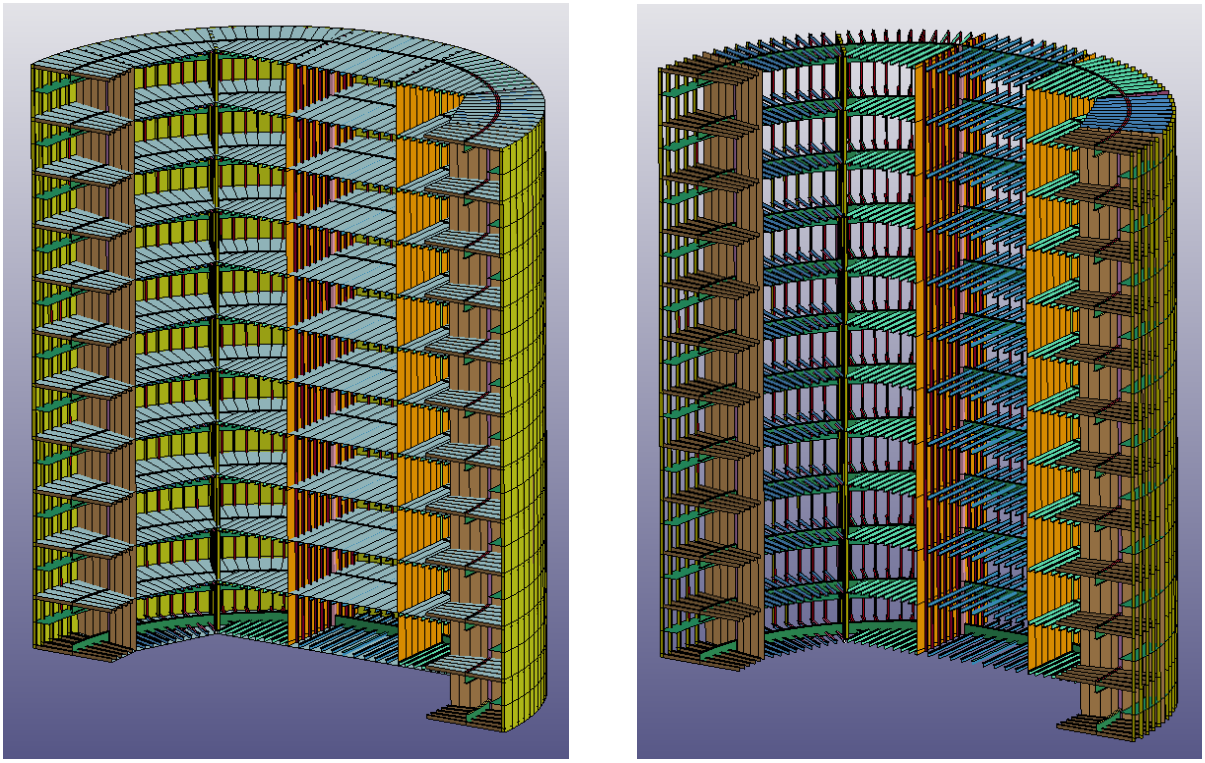

Figure 4.7: Pylon model and internal structure

4.3 Definition of the boundary conditions

Because the whole model has a large number of elements, the pylon was partially modeled depending on the collision direction, so in order to run the simulations half or a quarter of the model was used to decrease the computation time. The boundary conditions were considered fixed for the six degrees of freedom of the edge nodes. This assumption was applicable for all the computations.

4.4 Definition of the contact conditions

One of the key points to obtain more precise results is the contact definition between the pylon and the ship.

It will be understood that two bodies have been defined in the simulations, the first corresponds to the pylon and the second to the ship, at the same time the ship has been subdivided into two systems, one corresponding to the forecastle and the second corresponding to the bulb.

4.4.1 Surface to surface and single surface information

Contact input is required to define the interaction between the bodies. There are several options to be used in LS-DYNA. For this model, an automatic surface to surface was defined. The static (FS) and the dynamic coefficients (FD) of friction were set to 0.3. This input considers the frictional coefficients are dependent on the relative velocity LSTC (2006).

Extra shape and scaling information of the coefficients was defined by following the Supervisor's previous information.

4	SSID	MSID	SSTYP	MSTYP	SBOXID	MBOXID	SPR	MPR
	2	1	2	0	0	0	0	0
5	FS	FD	DC	VC	VDC	PENCHK	BT	DT
	0.3000000	0.3000000	0.0	0.0	0.0	0	0.0	1.000e+020
6	SFS	SFM	SST	MST	SFST	SFMT	FSF	VSF
	1.0000000	1.0000000	0.0	0.0	1.0000000	1.0000000	1.0000000	1.0000000

Figure 4.8: Automatic surface to surface input

Contact input was defined for self interaction of each body. The automatic single surface was defined as shown in fig.4.9. The FS and FD values were set to 0.35.

4	SSID	MSID	SSTYP	MSTYP	SBOXID	MBOXID	SPR	MPR
	2	0	2	0	0	0	0	0
5	FS	FD	DC	VC	VDC	PENCHK	BT	DT
	0.3500000	0.3500000	0.0	0.0	0.0	0	0.0	1.000e+020
6	SFS	SFM	SST	MST	SFST	SFMT	FSF	VSF
	1.0000000	1.0000000	0.0	0.0	1.0000000	1.0000000	1.0000000	1.0000000

Figure 4.9: Automatic single surface input

4.4.2 Initial design

The initial design considered a stiffening ring between the decks. Fig. 4.10 presents the back view of the original arrangement with one stiffening ring.

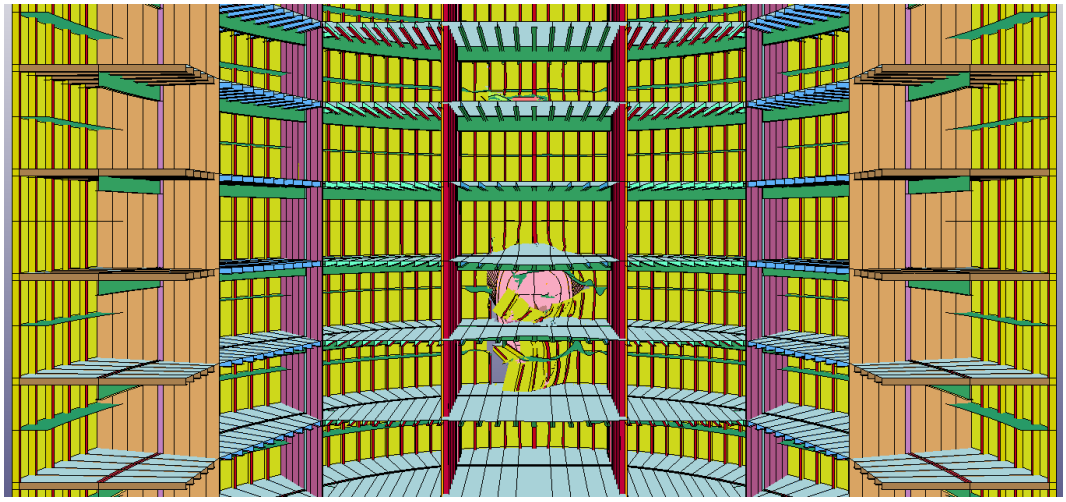

Figure 4.10: Back view considering one stiffening ring.

When the initial simulations were performed, the perimeter panel was vulnerable to being rapidly penetrated by the bulb. A single stiffening ring was not considered strong enough. Furthermore, the nearest area to the bulb was reinforced by adding two new extra stiffening rings. The new configuration is shown in fig. 4.11.

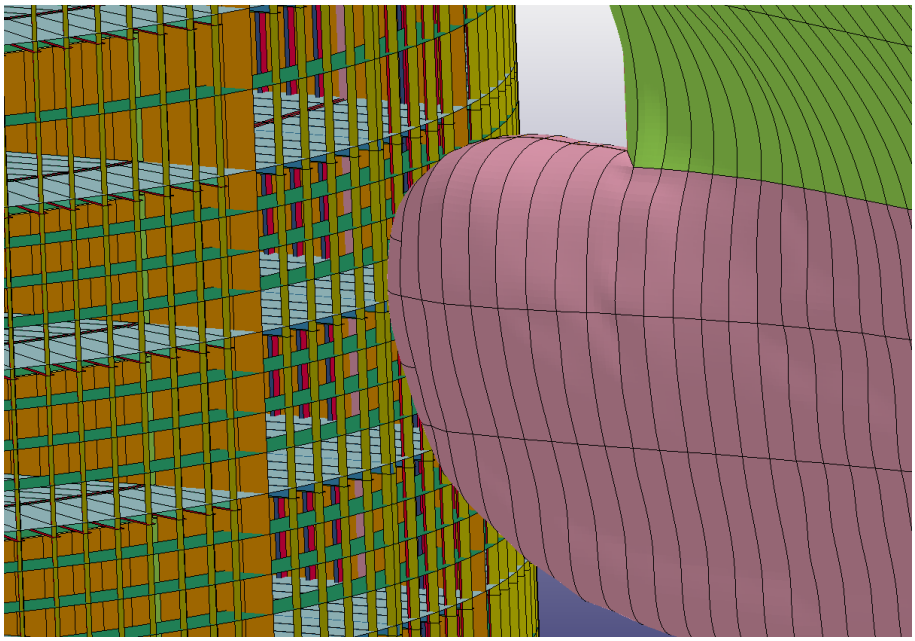

Figure 4.11: Back view of the panel after collision

4.5 Load cases selection and application

Three directions were simulated in LS-DYNA. These computations lasted 12 hours and a a collision time of 0.3 s was simulated. Figs. 4.12 to 4.14

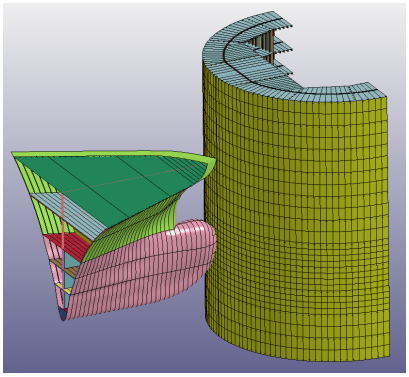

Figure 4.12: Collision 0°

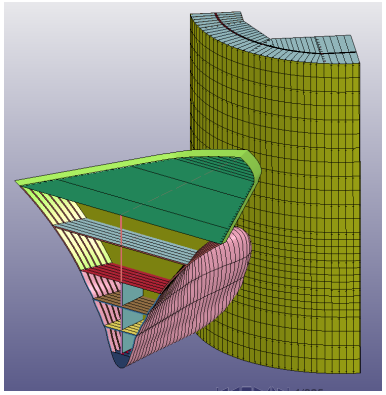

Figure 4.13: Collision 45°

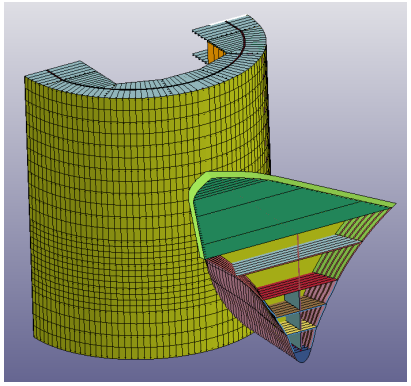

Figure 4.14: Collision 90°

The output information from this simulations was used to identify the structural performance and the estimated damage.

Chapter 5

LS-DYNA simulations and results

The total resultant force, the internal energy and the damage level expected for each scenario were calculated and compared, some modeling errors were identified and improved for subsequent simulations.

5.1 Initial resultant force

The relationship between the resulting force and time for the different collision scenarios was obtained from LS-DYNA. Firstly, fig. 5.1 compares the resultant force of the bulbous bow for diferent directions.

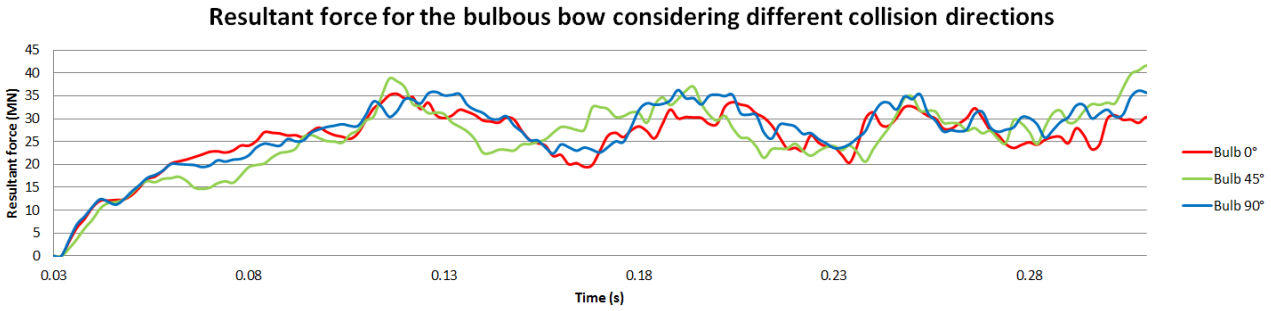

Figure 5.1: Resultant force for the bulbous bow considering different collision directions

According to the figure, the resultant force has slight variations when comparing different collision directions. This is associated to the specific failure mechanism. Due to these results

correspond to the initial design, the perimeter panel was penetrated by the bulb for the three directions.

The same analysis was executed for the forecastle, fig. 5.2 presents the same comparison.

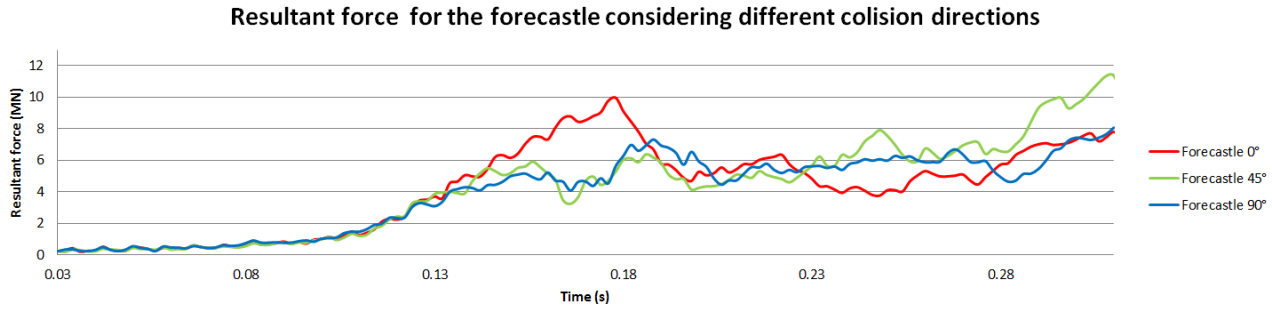

Figure 5.2: Resultant force for the bulbous forecastle considering different collision directions

The resultant force associated to the 0° direction is larger than the other directions from 0 to 0.18 s, however it slightly decreases to lower values after 0.18 s, the differences were not considerable.

5.2 Structural damage on the pylon

The structural damage is shown from fig 5.3 to 5.11 for all the scenarios. For all of the cases, both the ship and the pylon were damaged. The pylon was easily penetrated by the bulb and the forecastle.

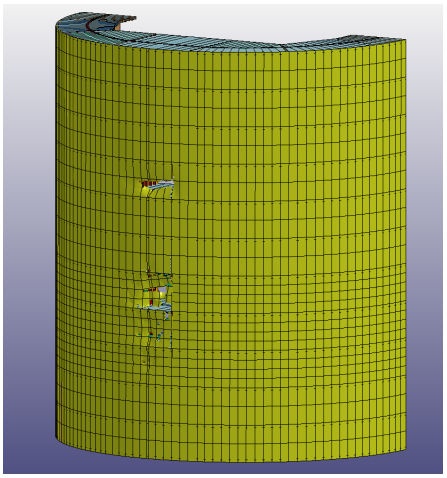

Figure 5.3: Pylon 0°

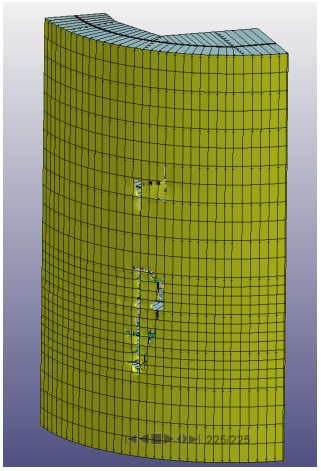

Figure 5.4: Pylon 45°

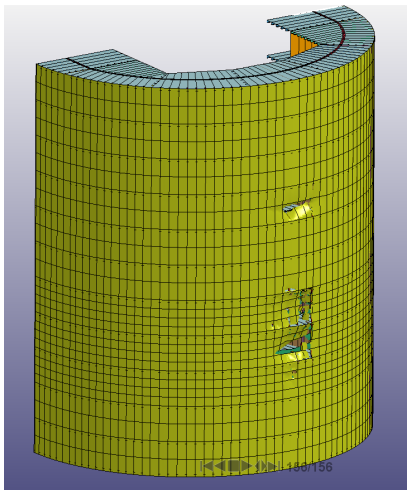

Figure 5.5: Pylon 90°

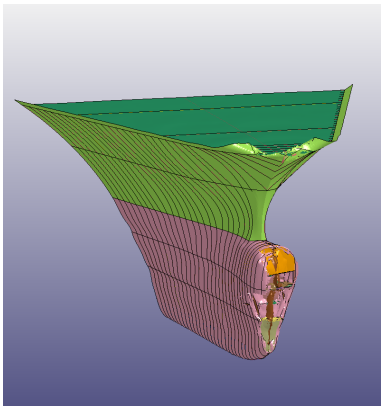

Figure 5.6: Ship 0°

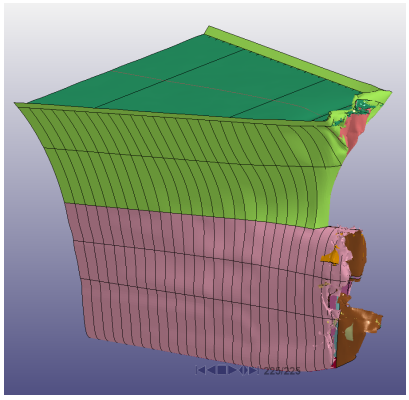

Figure 5.7: Ship 45°

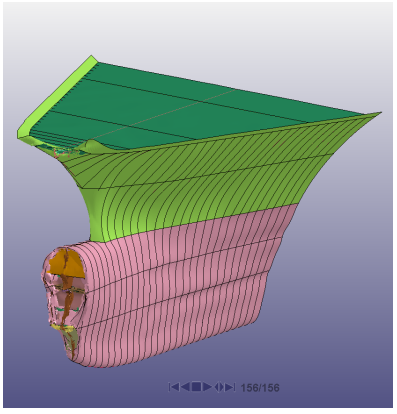

Figure 5.8: Ship 90°

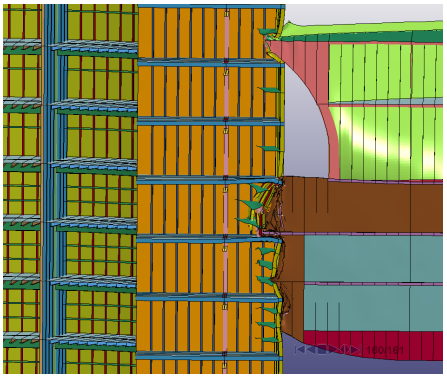

Figure 5.9: Lateral view 0

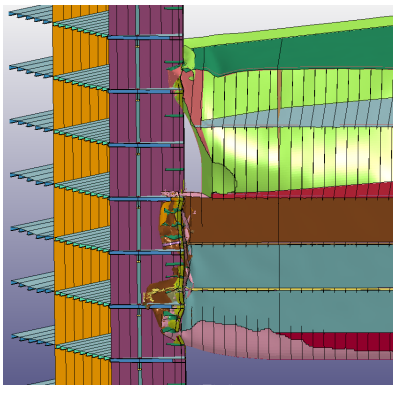

Figure 5.10: Lateral view 45

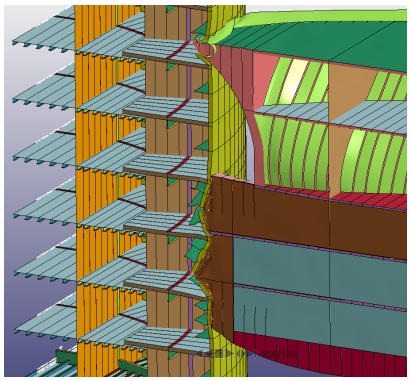

Figure 5.11: Lateral view 90

The design of the pylon was submitted to redesign and reinforcement to decrease the damage level. The expected number of flooded compartments in relation to the collision direction was identified with these approach. For a ship collision perpendicular to the bridge, three compartments were flooded, while 6 compartments for 45° and three for 90 °.

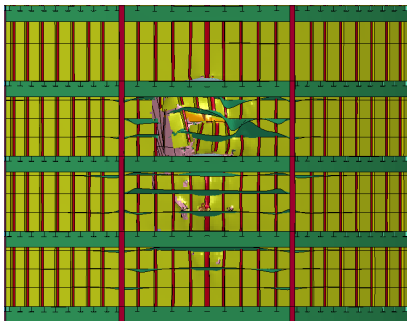

Figure 5.12: Back view 0 °

Figure 5.13: Back view 45 °

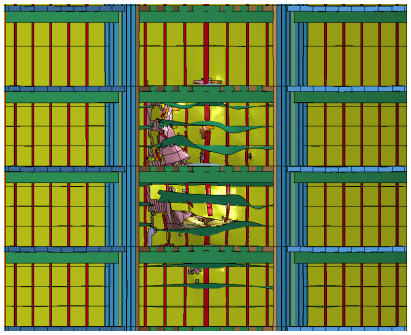

Figure 5.14: Back view 0 °

The importance of identifying the damage for the pylon is to estimate the extra loads due to flooded compartments and the influence on the stability. This estimation is included in subsequent analysis in USFOS.

5.3 Total internal energy comparison between the ship and the pylon

The total internal energy was obtained from LS-DYNA by summing up the internal and the eroded internal energy of the ship and the pylon. Fig. 5.15 compares the results from this analysis.

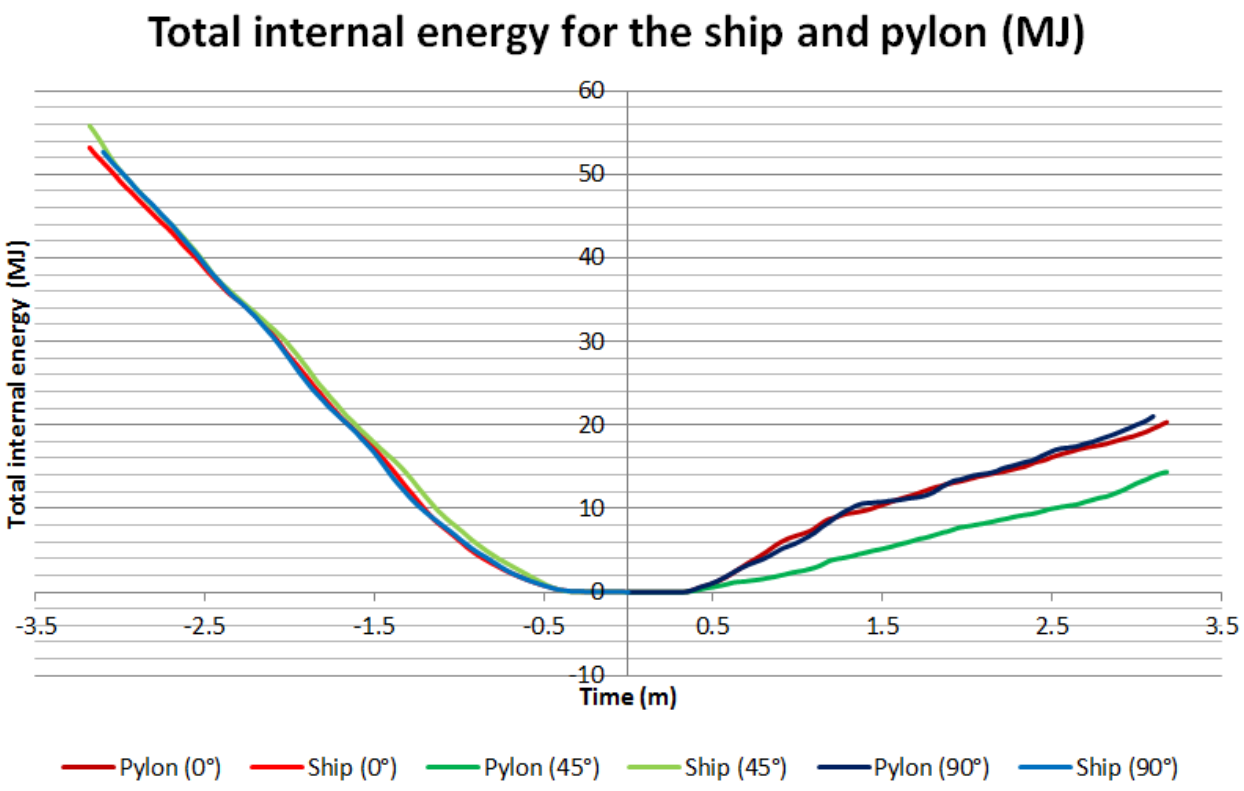

Figure 5.15: Resultant force for the bulbous bow considering different collision directions. Note: The x axis is positive for both sides

The internal energy is compared in terms of the different collision directions. The energy of the ship is on the left side and the energy associated to the pylon is on the right side. It might be seen that for all of the cases the internal energy is larger for the ship.

On the other hand, when comparing the same body for different scenarios, the internal energy for the ship remains similar for all of the directions. However the energy of the pylon decreases considerably for the 45° collision, this is associated to the existing bulkhead which increases the strength.

5.4 Redesign of the pylon

Based on the above results, a redesign of the pylon was carried out. Therefore, steel properties and the thicknesses of the plates for different elements were modified to increase the structural strength.

First the pylon was modified by strengthening the steel, NV A36 with a a yield stress equal to 355 MPa. The material parameters are contained in table 5.1, .

Table 5.1: Material properties for the redesign

Steel properties for the Pylon Steel NV A36								
γ	E	ν	G	B	σ_y	K	n	eps
kg/m3	Pa	–	Pa	Pa	Pa	Pa	–	–
7850	2.1E11	0.3	7.96E10	1.73E11	3.55E8	8.76E8	0.157	0.005
Steel properties for the ship Steel S275								
γ	E	ν	G	B	σ_y	K	n	eps
kg/m3	Pa	–	Pa	Pa	Pa	Pa	–	–
7850	2.1E11	0.3	7.96E10	1.73E11	2.75E8	8E8	0.161	0.005

Two new models with increased plate thicknesses were proposed. Hereinafter, the dimensions and results of the original model are identified as "original", while the reinforced models correspond to "Sim1" and "Sim2". The thicknesses used for all the structural elements of the different models are shown in the following table 5.2. The thickness increment is observed for the models Sim1 and Sim2.

Table 5.2: Plates thickness of the original and redesigned models

Section	Definition	Original (mm)	Sim1 (mm)	Sim2 (mm)
1	Web girders compartment 1	9.7	10.9	11.6
2	Flange girders compartment 1	16	18	18
3	Web girders compartment 2	9.7	10.9	11.6
4	Flange girders compartment 2	16	18	18
5	Web girders compartment 3	9.7	10.9	11.6
6	Flange girders compartment 3	16	18	18
7	Web girders compartment 4	9.7	10.9	11.6
8	Flange girders compartment 4	16	18	18
9	Web vertical stiffeners	10.5	12.5	12.5
10	Flange vertical stiffeners	14	16	18
11	Web stiffeners bulkhead 1	10.5	12.5	12.5
12	Flange stiffeners bulkhead 1	14	16	16
13	Web stiffeners bulkhead 2	10.5	12.5	12.5
14	Flange stiffeners bulkhead 2	14	16	16
15	Web stiffeners bulkhead 3	10.5	12.5	12.5
16	Flange stiffeners bulkhead 3	14	16	16
18	Web beam	15.75	15.75	15.75
19	Superior flange	27.69	27.69	27.69
20	Inferior flange	27.69	27.69	27.69
21	Bottom plate	14	18	22
22	Ring plate	14	18	22
23	Perimeter plate	16	18	22
24	Bulkhead 1 plate	16	16	16
25	Bulkhead 2 plate	16	16	16
26	Bulkhead 3 plate	16	16	16
29	HSS bulkhead 1	9.5	9.5	9.5
31	HSS bulkhead 2	9.5	9.5	9.5
33	HSS bulkhead 3	9.5	9.5	9.5

New collision simulations were performed considering the thicknesses above. Firstly, fig. 5.16 to 5.18 visualizes the lateral views for the original model, a range of time equal to 0.9 s was simulated for the following computations.

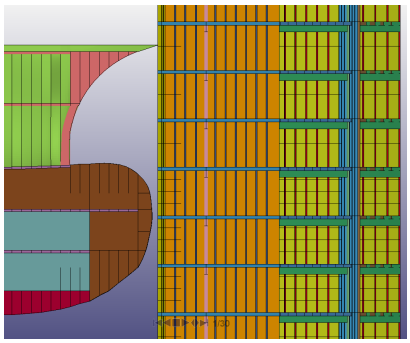

Figure 5.16: Time=1 s

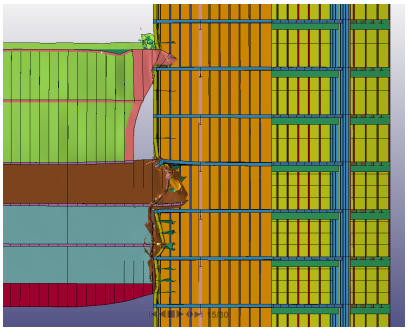

Figure 5.17: Time=0.42 s

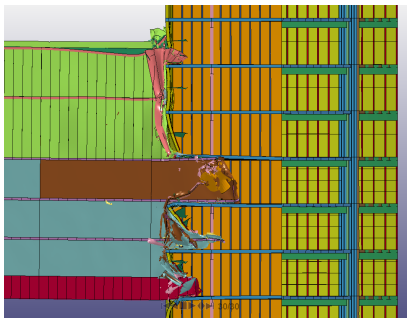

Figure 5.18: Time=0.87 s

Based on the last results, the original design was considered weak, the bulb fully penetrates the pylon, causing considerable damage to the perimeter panel, the outer plate was easily penetrated and the stiffeners presented important deformations. The ship bow presented considerable damage as well but the pylon damage was not acceptable.

Similarly, lateral views are shown for the collision simulation considering the reinforced model Sim1.

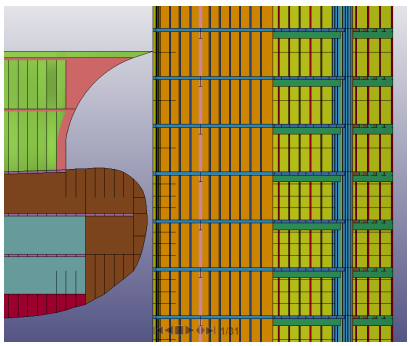

Figure 5.19: Time=1 s

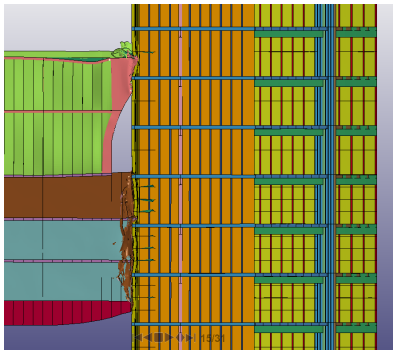

Figure 5.20: Time=0.42 s

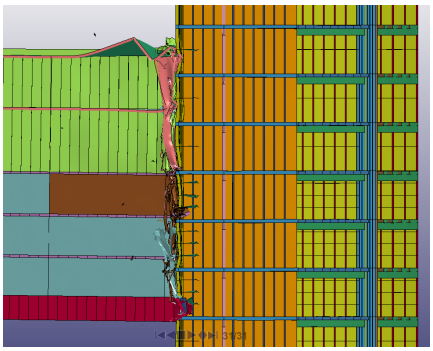

Figure 5.21: Time=0.90 s

Most of the damage was concentrated on the forecastle and bulb, since this was considerably shrunken. Overall, the pylon had less damage.

Finally the reinforced model Sim2 is presented.

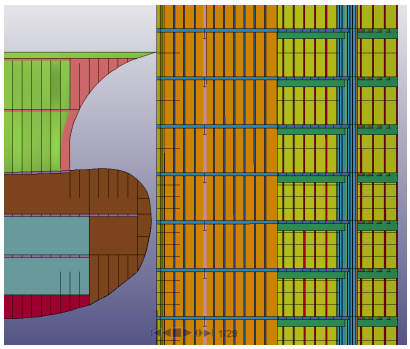

Figure 5.22: Time=1 s

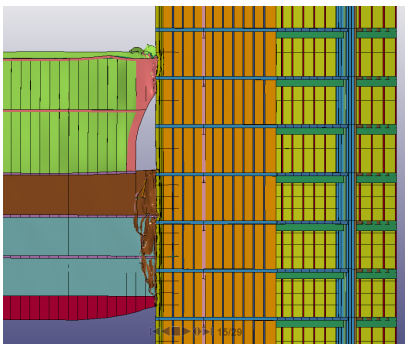

Figure 5.23: Time=0.42 s

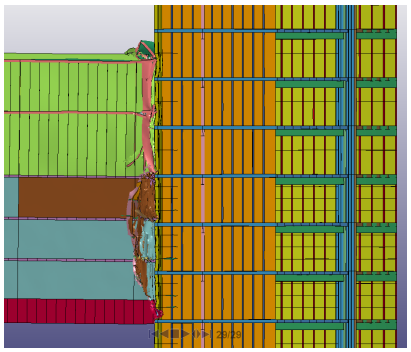

Figure 5.24: Time=0.84 s

Finally the reinforced model Sim2 presented minimum damage for the pylon,, the ship was shrunken along the whole simulation and the deformations dropped to minimum values. This model was considered too conservative for this vessel.

5.5 Hourglass verification

Based on the empirical recommendations from the supervision, the hourglass energy should be kept under a maximum value of 10% of the internal energy. When defining the hourglass for the simulation, the selected value was defined as 4. The initial simulations considered a value of 1, however the hourglass values were over the limiting ratio of 10%.

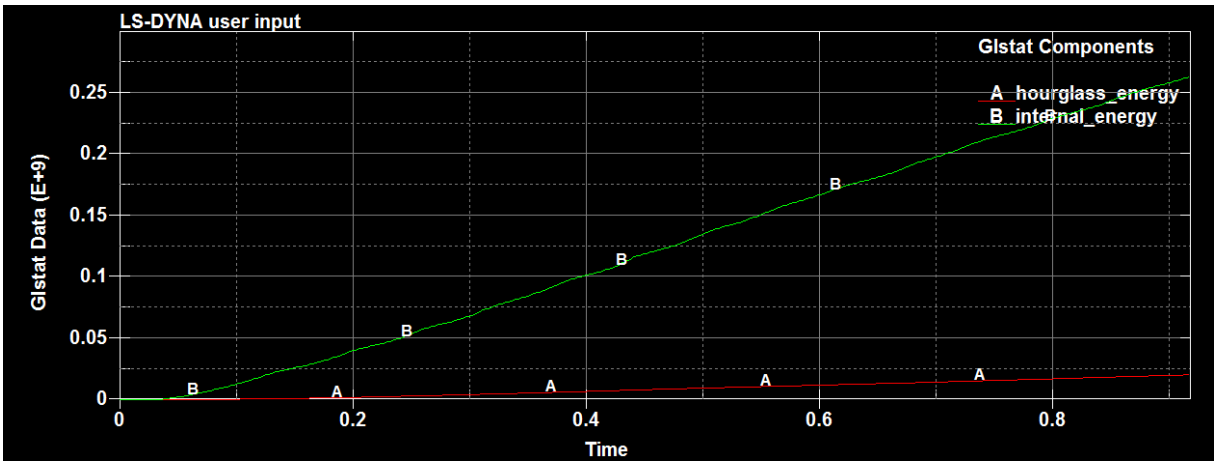

Figure 5.25: Hourglass verification

The hourglass and the internal energies are shown in fig. 5.25.

5.6 Selected design for the pylon

The energy of the ship is plotted on the left side and the energy associated to the pylon is on the right side. The internal energy of the ship is larger for all of the cases.

When analyzing the plot, a pattern is identified. For the strongest design, the internal energy of the ship increases, while weaker pylons would take more energy. There is a considerable difference in energy between the original and the redesigned models Sim 1. However, the difference is not considerable between the models Sim1 and Sim2.

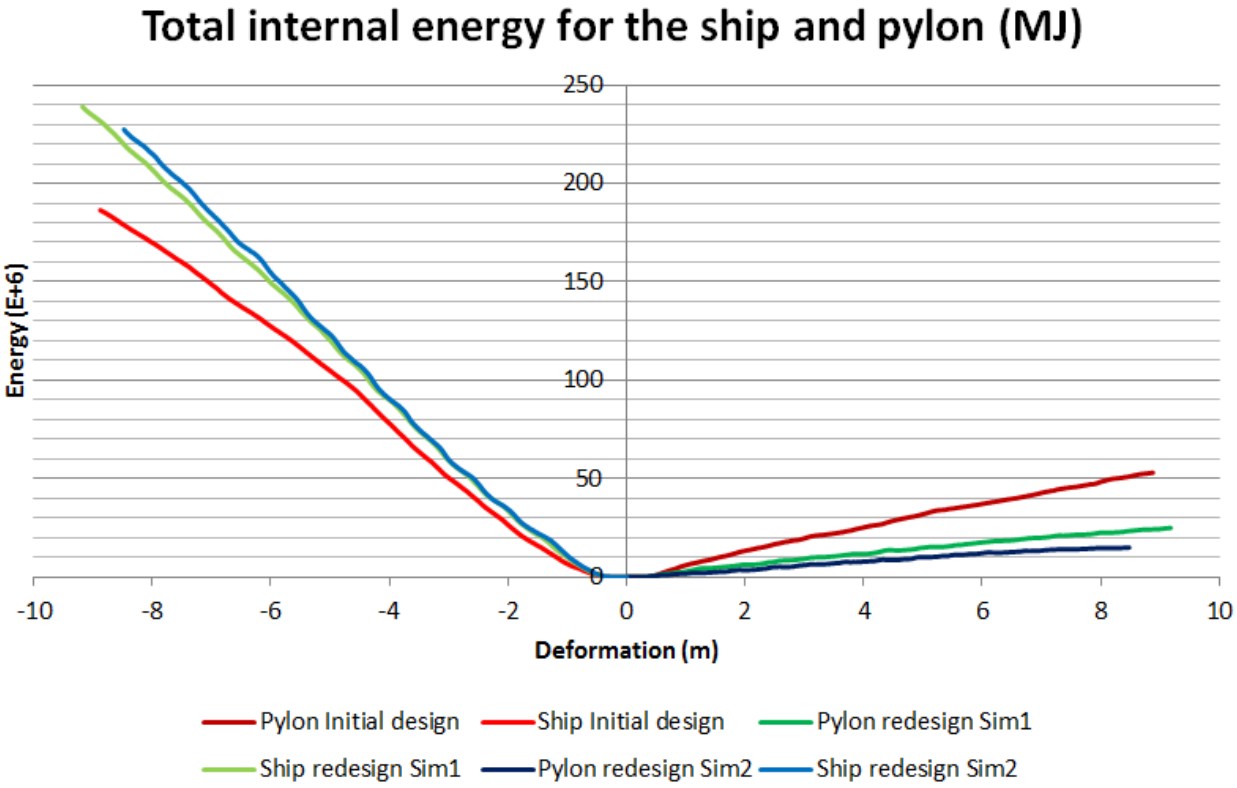

Figure 5.26: Total internal energy for the ship and pylon

The damage level is graphically compared for both structures by using LS-DYNA 3D plots in fig. 5.27. The bulb and the forecastle are shrunken after the collision; on the other hand, the

pylon is barely damaged. This view corresponds to the reinforced model Sim1.

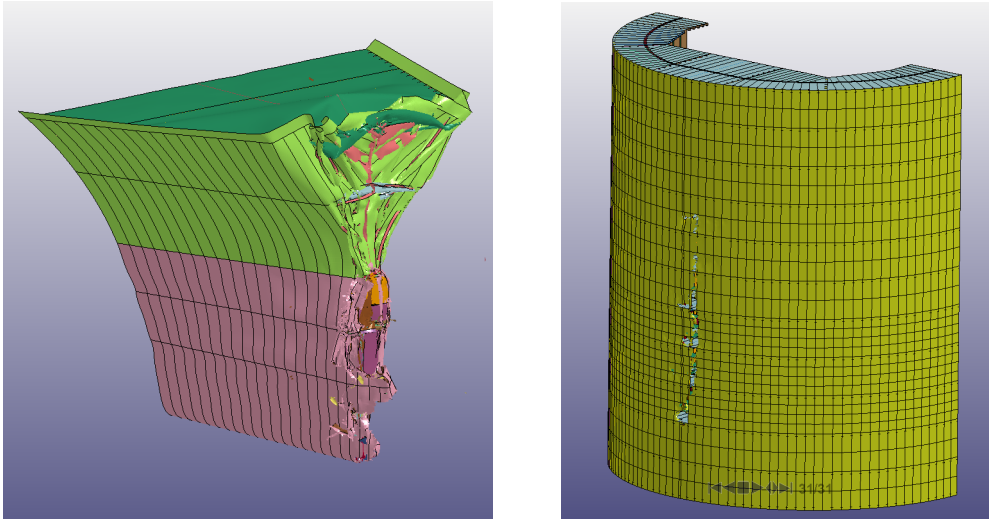

Figure 5.27: Structural damage for the collision

5.7 Force displacement curves

The resultant forces for the three models were obtained from LS-DYNA computations and simple post-processing. Fig.5.28 presents the force-deformation curve for the bulb and the forecastle related to the original model. The force of the bulb is higher than the force of the forecastle for the three models and a maximum value of 39.4 MN is reached

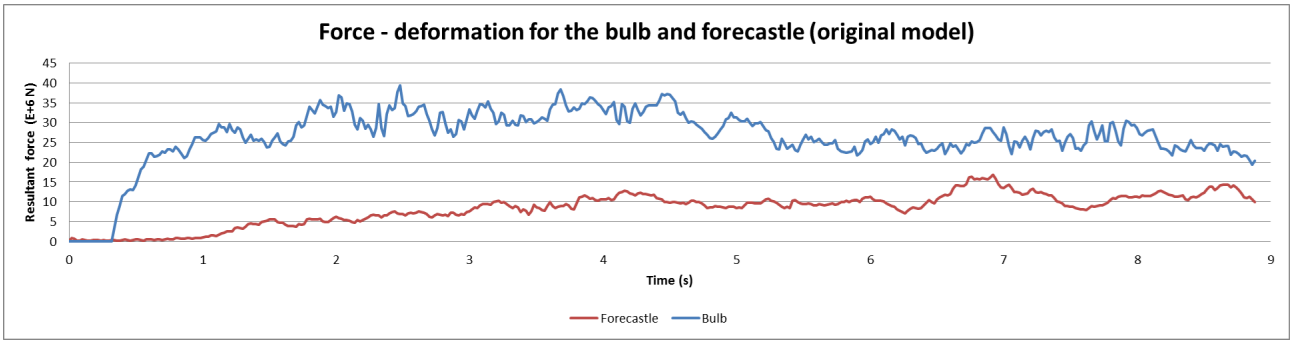

Figure 5.28: Force-deformation for the bulb and the forecastle (Original model)

In fig. 5.29 when analyzing the force deformation curve of the reinforced model Sim1, considerable fluctuations between 16.1 MN and 47.2 MN were identified for the bulb. This variation

might be associated to fluctuating contact areas due to the failure of the ship elements.

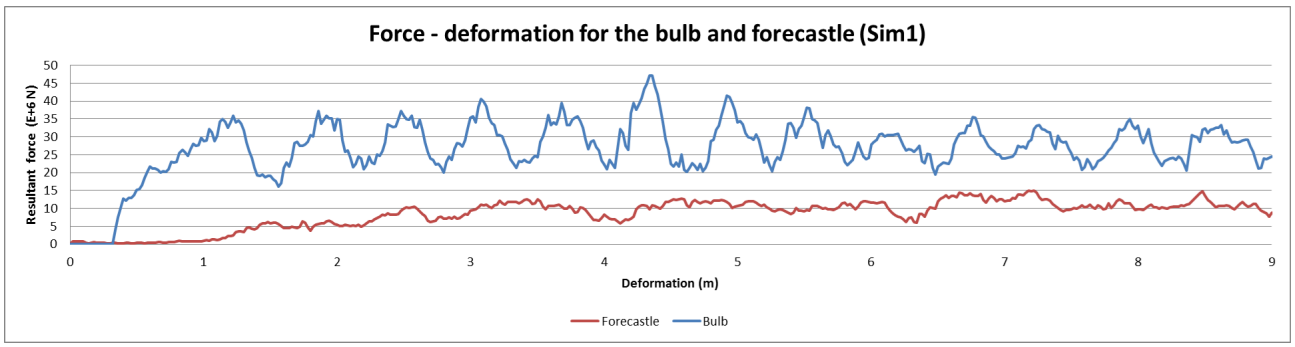

Figure 5.29: Force-deformation for the bulb and the forecastle (Sim1)

Following a similar analysis for the Model Sim 2, fluctuations between 50.3 MN and 15 MN were identified. For the three models the force of the forecastle remains with slight changes.

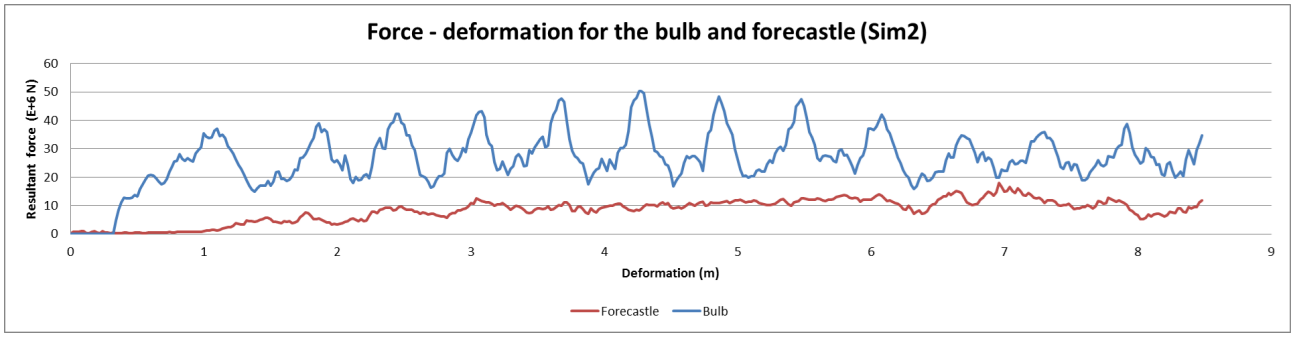

Figure 5.30: Force-deformation for the bulb and the forecastle (Sim2)

Fig. 5.31 compares the force-deformation curves of the bulb for the three models. A similar behavior for models Sim1 and Sim2 was identified, the reason is that a similar ship failure dominates both simulations, on the other hand, both structures fails in the original model.

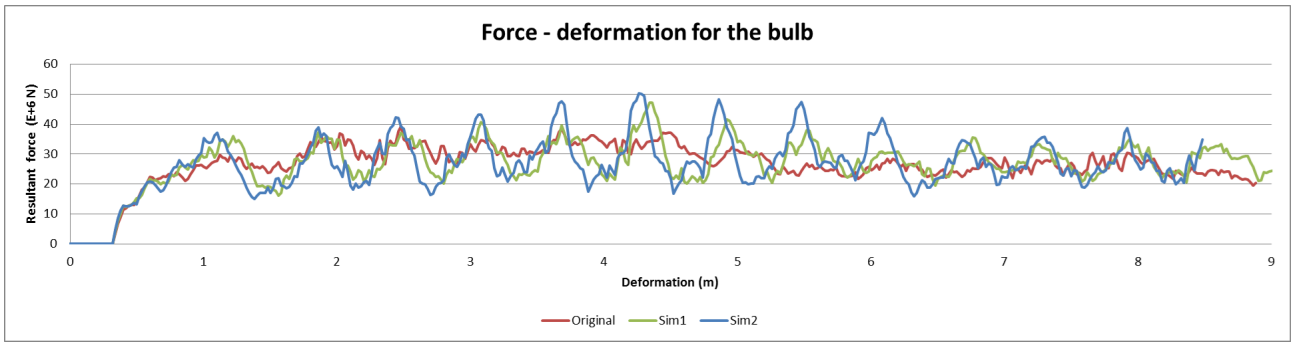

Figure 5.31: Force-deformation comparison for the bulb

A similar analysis of the forecastle demonstrates that the force variation is less significant.

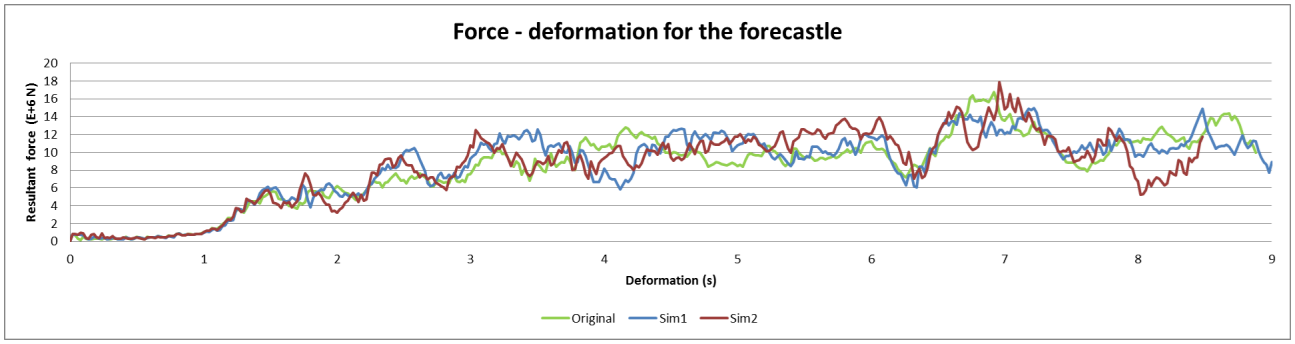

Figure 5.32: Force-deformation comparison for the Forecastle

Recommended 3D visualizations are included in Appendix 3, some plots associated to the contours of resultant moments, normal forces, stresses, strains, pressure, thickness and displacements are included for the reader to understand the failure mechanism.

5.7.1 Collision against a rigid wall

Previous collision simulations were conducted by Sha Y., the simulationes considered collisions against a rigid wall. Later, the results were provided to compare with the final design of the pylon.

Fig. 5.33 compares the resultant force between the model Sim1 and the results from ship collision with a rigid wall.

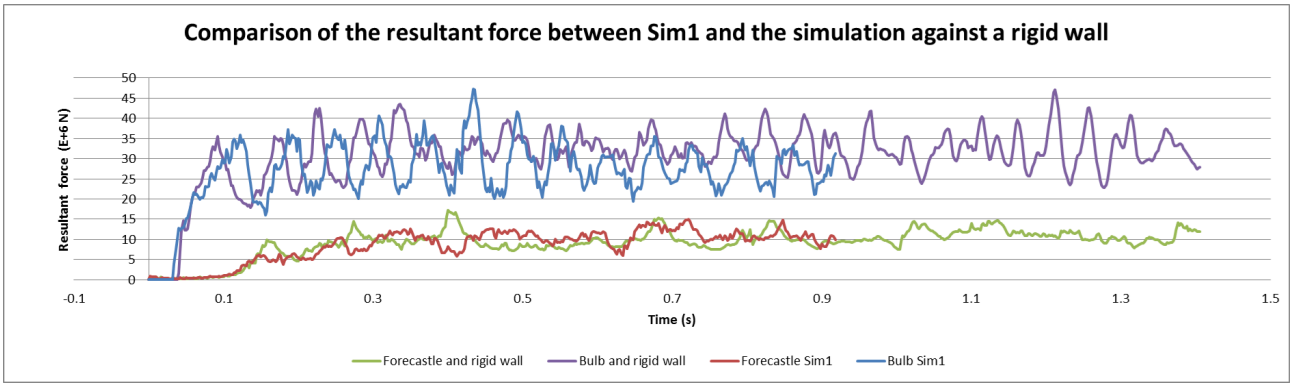

Figure 5.33: Comparison of the resultant force between the Sim1 and a rigid wall

According to the figure, both the bulb and the forecastle of the final design have similar collision responses when compared with the collision against a rigid wall. The rigid wall simulations lasted longer, however a similar behavior is expected for the model Sim1.

Chapter 6

Ship collision modelling using USFOS

This chapter describes the modeling of the dynamic response of the bridge considering accidental loads due to ship collision. For this simulation, the model proposed by Harald O. (2016) was used in combination with the LS-DYNA results.

6.1 Background

The Bjørnefjorden TLP bridge is a 3-span suspension bridge with floating pylons fixed by tension legs. The Bjørnefjor is 5 km wide at the narrowest so the project considers a length of 1385 m for each span.

The side spans consider 300 m for the south side and 353 for the north side. Considerable depths of the fjord reach about 550 m at one of the floaters and 450 m for the other. Fig. 6.1 shows the lateral drawing provided by the supervision.

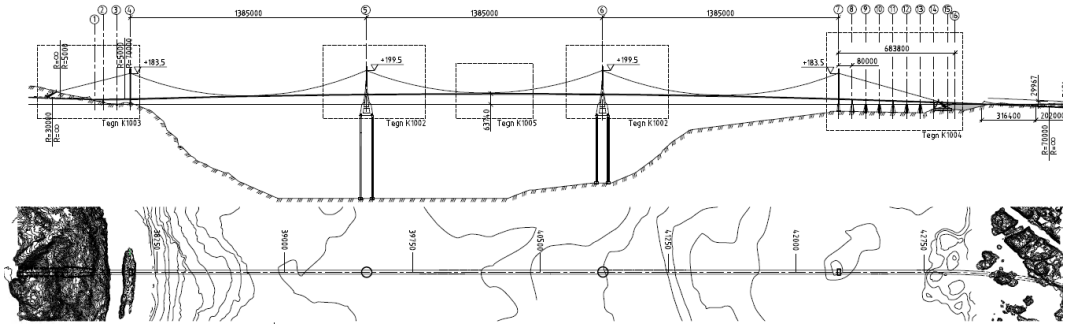

Figure 6.1: Bridge lateral drawing, Jørgen Amdahl (2017)

6.2 Brief description of the bridge model

The Bjørnefjorden TLP Supported Bridge is a floating structure. The deck is supported by hangers connecting the deck to the main suspenders hanging between the towers. Fig. 6.2 introduces an isometric view of the USFOS model built by Harald O.

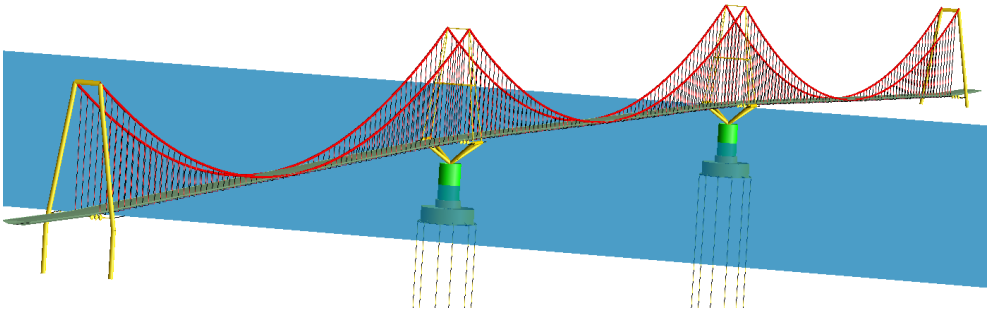

Figure 6.2: USFOS model by Harald O.

For suspension bridges, the deck loads are transmitted to the suspenders through the hangers and later to the towers. The towers transmit the forces vertically to the pylons which reach hydrostatic equilibrium.

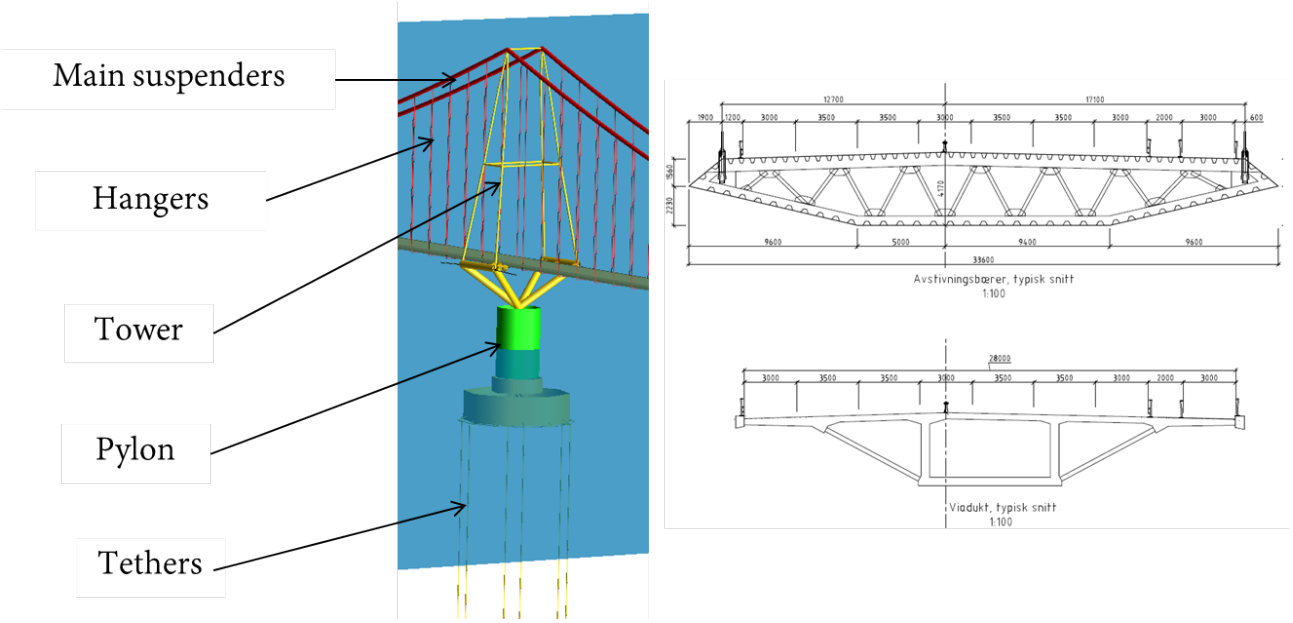

Figure 6.3: Floating towers and decks section

The floating towers is shown in fig. 6.3. The pontoon is connected to the seafloor with tethers. At the same time the tower rises from the pontoon with beam elements.

On each end side, the bridge is supported by towers which are the superstructure onshore. Fig. 6.4 illustrates the onshore superstructure and the drawings of the towers. For the original model, the suspenders connect directly to the highest points, but not passing beyond the superstructure to the deck level onshore.

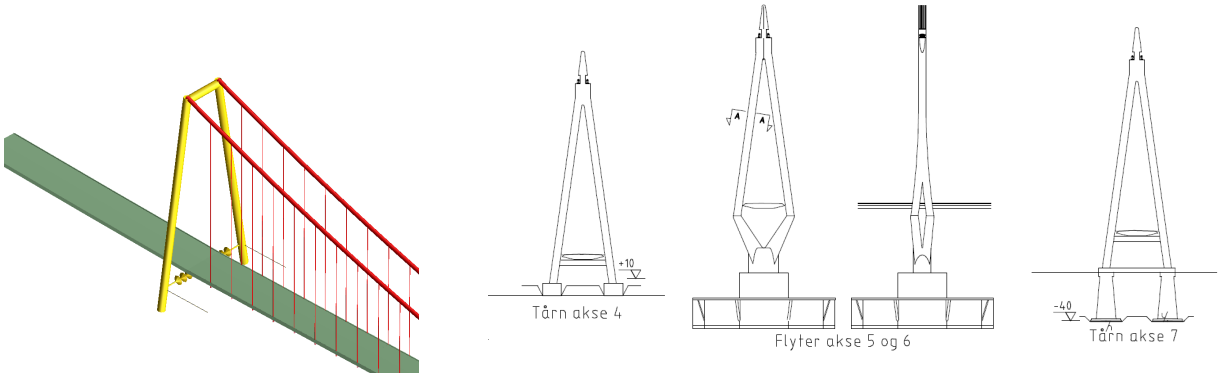

Figure 6.4: Towers model and drawing

A top view of the tower and the isometric view of the floating hull is illustrated in fig. 6.5.

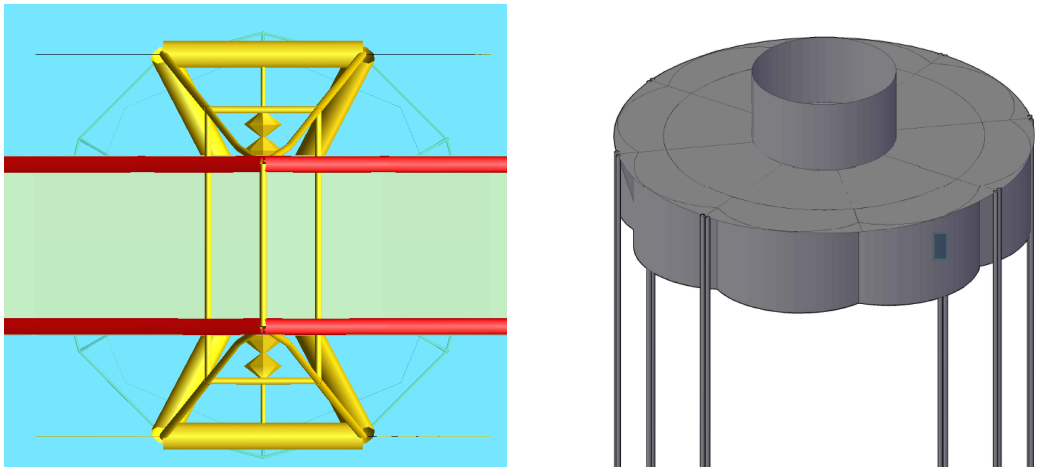

Figure 6.5: Left: Top view of the model. Right: Isometric sketch of the floating pylon

6.3 Selection of control nodes

Control nodes were proposed to study the dynamic response of the bridge as shown in fig. 6.6. Maximum displacements, velocities and accelerations were registered and compared. The nodes were selected following the same nodes from Harald O. (2016) as reference.

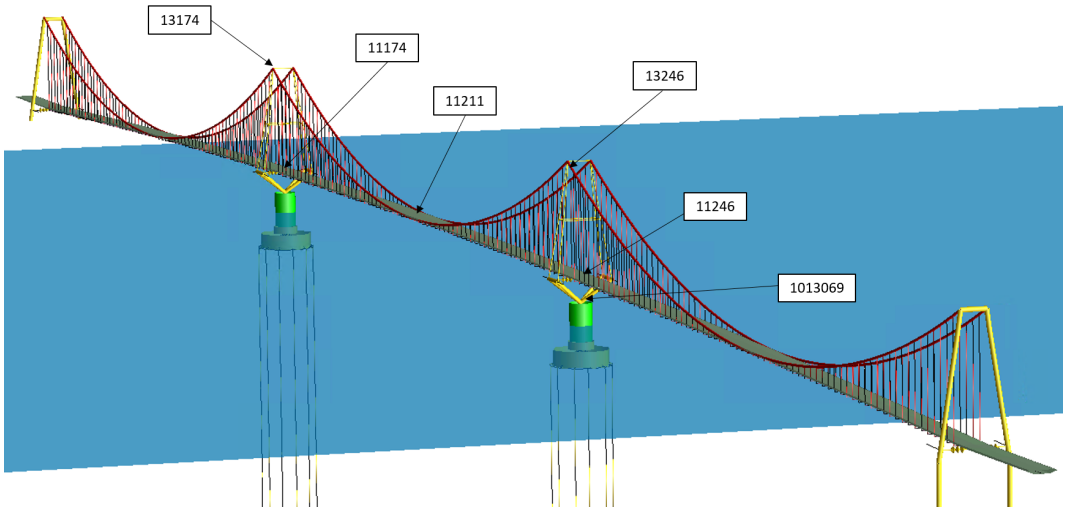

Figure 6.6: Selection of the control nodes

Nodes 11174 and 13246 correspond to the highest point of the towers, 11174 and 11246 are located on the bridge deck above the center of the floaters while node 1013069 is located on the upper bound of the floater, finally node 11211 is located on the longitudinal center of the bridge between the two pylons.

6.4 A brief introduction to USFOS

According to the designers, the goal of USFOS is to conduct ultimate resistance analysis and progressive collapse of offshore structures. To perform the analysis, the structure is set by beam elements.

According to Jørgen Amdahl (1988), by implementing accidental loading as a category in design regulations of offshore structures, there was also the need to implement new and more advanced tools that allowed these analyzes to be carried out. Given the nature of these struc-

tures, it is of interest to know the damage level after collision, as well as the residual resistance. This is when USFOS finds considerable applications.

In order to familiarize the reader with the implemented algorithms in USFOS, it is recommended to use the theoretical manual of the software, which presents step-by-step analysis methods, iteration balance, arc length control, among other topics.

6.4.1 Updated ship force-deformation

As a result of the simulations in LS-DYNA, the force-time curve was obtained. Fig. 6.7 ilustrates the resultant force relation along the simulated time.

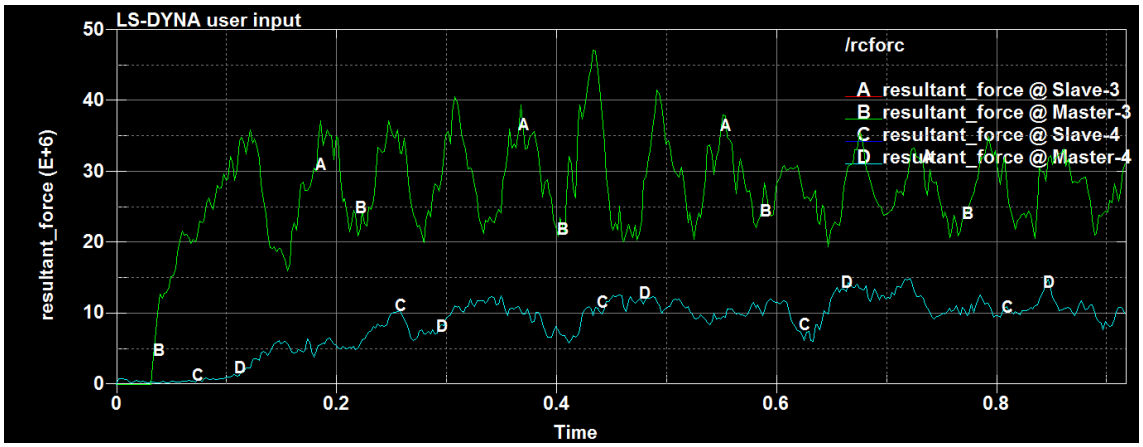

Figure 6.7: Resultant force

The resultant force related to the bulb is shown in green color, while the resultant force of the forecastle in blue along a simulated time of 0.9 s.

By dividing the time axis by the velocity of the ship used for the simulation (10 m/s), the resultant force-displacement was obtained as shown in fig. 6.8 which considers the resultant force of the bulb.

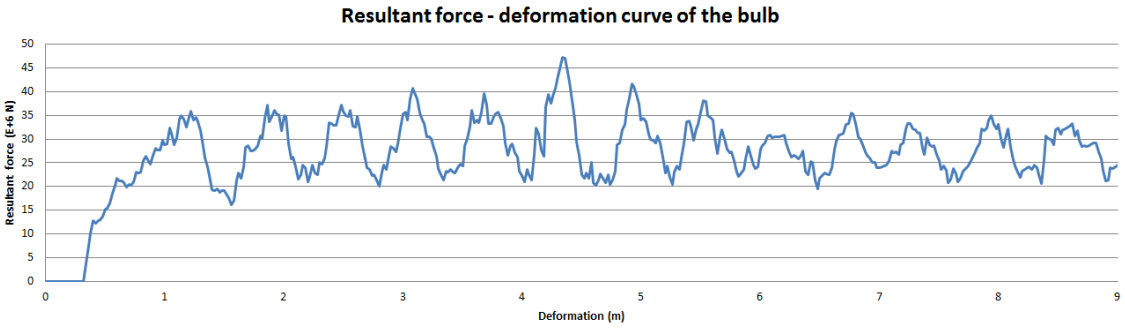

Figure 6.8: Simulated force deformation curve from LS-DYNA

A simplified force - deformation curve of the bulb is shown below.

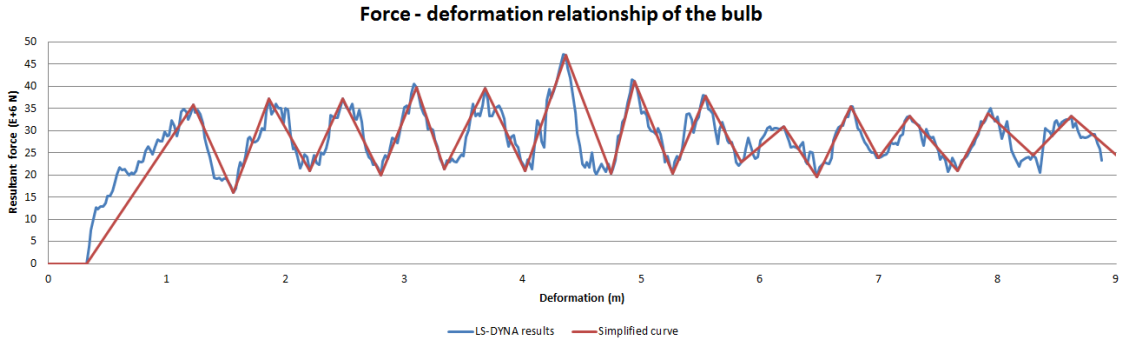

Figure 6.9: Simplified force deformation curve

By using the last curve, USFOS simulations were consudted to study the dynamic response.

6.4.2 Central impacts analysis considering the bulb

A mass and a nonlinear spring were implemented to simulate the ship collision effects. The following figure illustrates the proposed system.

Firstly a nonlinear spring is represented by element 2 which takes into account the force-deformation relationship from LS-DYNA; while element 3 represents a hyperelastic spring implemented to bounce the ship back after the collision. A nodal mass of 16905 tonnes representing the ship is applied to node number 2 which considers a velocity of 11.3 m/s (22 knots). Fig. 6.10 presents the spring system to analyze the pylon.

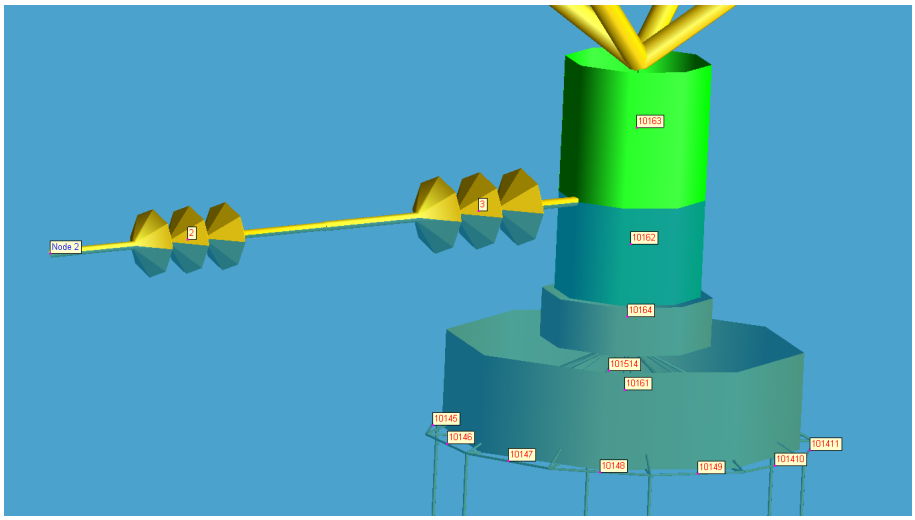

Figure 6.10: Spring system for the bow collision

Bridge displacements considering only the bulb

When the simulation was finished, a maximum lateral displacement of 15.23 m was identified for the control point. According to fig. 6.11.

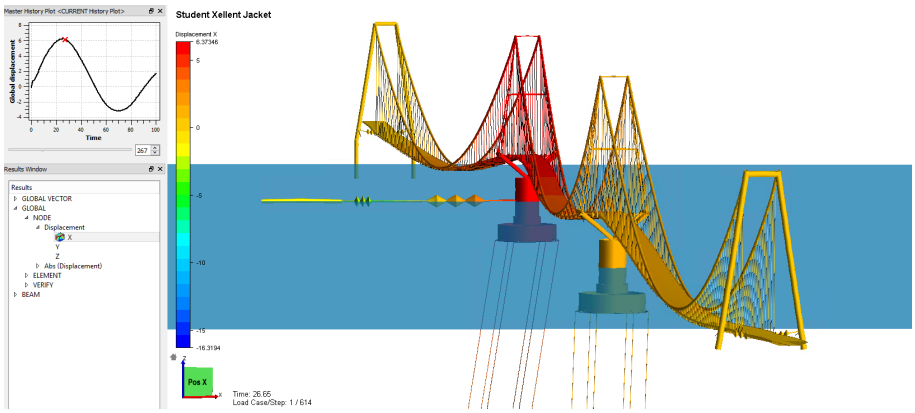

Figure 6.11: Lateral displacements in USFOS.

After the collision, the ship is bounced back and the pylon reaches a negative displacement as shown in fig. 6.12. According to the result, the bridge would displace about -9.44 m along the x axis.

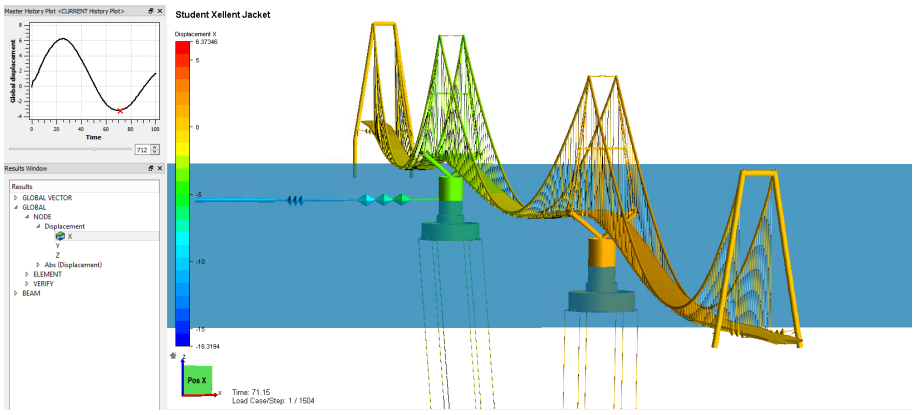

Figure 6.12: Negative lateral displacement in USFOS.

The maximum and minimum displacements, accelerations and the element forces are shown in table 6.1.

Table 6.1: Displacements, accelerations and forces under the collision simulation.

Maximum displacements and accelerations for tower 1				
Item		Units	Min	Max
Floater 1	Displacement Bridge Girder	[m]	-9.44	15.232
	Acceleration Bridge Girder	[m/s2]	-3.86	2.27
	Displacement Tower	[m]	-9.49	15.515
	Acceleration Tower	[m/s2]	-6.53	3.13
Maximum displacements and accelerations for tower 2				
Floater 2	Displacement Bridge Girder	[m]	-6.43	6.85
	Acceleration Bridge Girder	[m/s2]	-0.52	0.50
	Displacement Tower	[m]	-6.43	6.88
	Acceleration Tower	[m/s2]	-0.17	0.20
Maximum forces for selected members				
Cable Force		[MN]	129	135
Tether Force	N10131	[MN]	11.57	-68.9
Tether Force	N10231	[MN]	39.79	-22.96

6.4.3 Central impacts analysis considering the bulb and the forecastle

. The simulations were extended to include the effects of the forecastle. Thus the model was modified by adding a second spring representing the second force deformation curve. Fig. 6.13 shows simplified force-deformation curves for the forecastle.

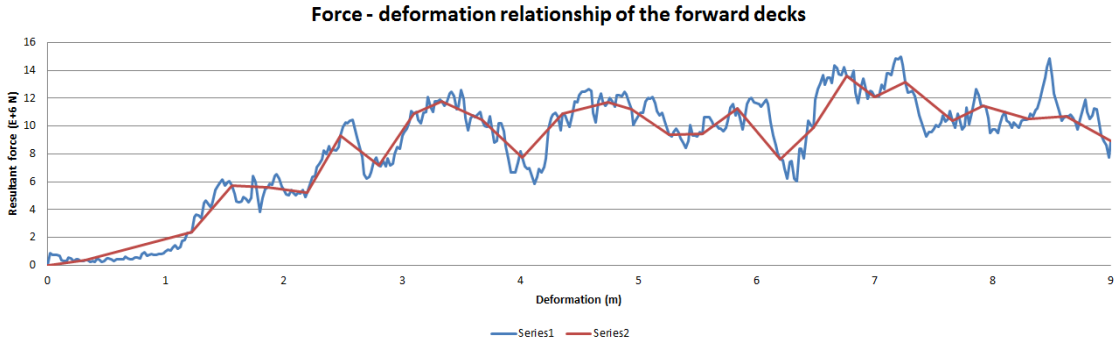

Figure 6.13: LS-DYNA and simplified force-deformation curves for the forecastle.

Bridge displacements considering the bulb and forecastle

The model was modified to take into account the effect of the two force-deformation curves from LS-DYNA. A parallel spring system was modelled 10.5 m. above the bulb coordinate to represent the forecastle. Fig. 6.14 illustrates the modification.

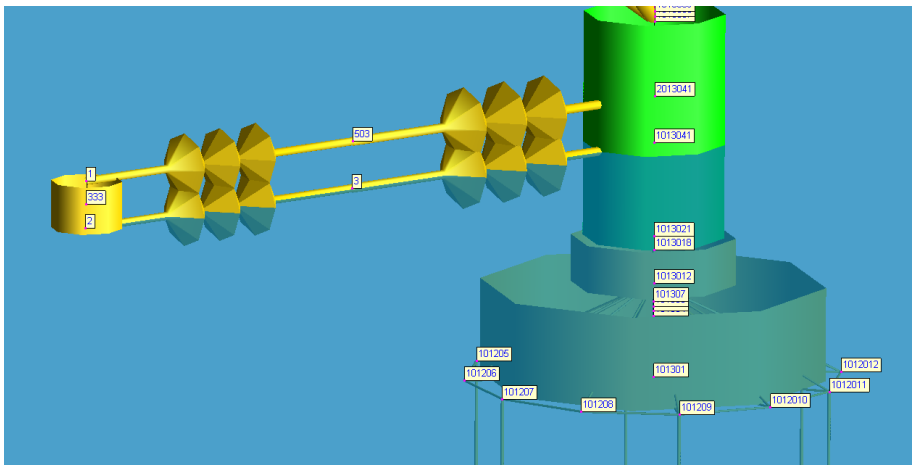

Figure 6.14: Spring system considering the bulb and the forecastle.

To model the effect of the springs accurately, both spring systems are connected to the column considering the dimensions of the ship. Both springs were connected to a rigid element on

the left side where the mass and the initial velocity are assigned. A maximum lateral displacement of 14.44 m was identified for the control point, there was a slight decrease. The displacements, accelerations and forces for this simulations were registered in table 6.2.

Table 6.2: Displacements, accelerations and forces under the collision simulation.

Maximum displacements and accelerations for tower 1				
Item		Units	Min	Max
Floater 1	Displacement Bridge Girder	[m]	-7.54	14.44
	Acceleration Bridge Girder	[m/s2]	-1.78	2.21
	Displacement Tower	[m]	-7.50	14.43
	Acceleration Tower	[m/s2]	-2.72	3.35
Maximum displacements and accelerations for tower 2				
Floater 2	Displacement Bridge Girder	[m]	-7.93	6.78
	Acceleration Bridge Girder	[m/s2]	-0.08	0.11
	Displacement Tower	[m]	-6.77	6.79
	Acceleration Tower	[m/s2]	-0.23	0.27
Maximum forces for selected members				
Cable Force		[MN]	130	135
Tether Force	N10131	[MN]	8.03	-47.8
Tether Force	N10231	[MN]	31.8	-24.6

Chapter 7

Residual strength analysis of the bridge

7.1 Collisions damage description

In Chapter 4 the damage to different collision scenarios. In all scenarios, the bulb penetrated the outer plate of the pylon. In this situation, the possibility of flooded compartments of the pylon was considerably high, so the effect of the flooded volumes were studied.

7.2 Flooding of compartments effects

According to the simulations, when the collision occurs perpendicular and in parallel to the bridge, three compartments are damaged, therefore the corresponding volume is considered flooded for both cases.

On the other hand, when the collision occurs with a 45° orientation, the damage occurs in six compartments.

The volumes were estimated and included in the USFOS model as concentrated forces. Fig. 7.1 presents the volumes associated to every compartment.

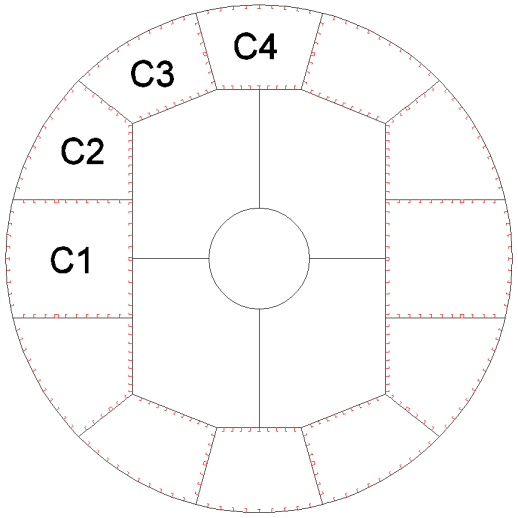

Flooded volumes		
	Area m^2	Volume m3
C1	30.70	92.1
C2	30.56	91.68
C3	34.96	103.9
C4	25.75	77.25

Figure 7.1: Flooded volume per compartment

Considering the number of damaged compartments associated to different collision directions, the calculation of extra masses is shown in Table 7.1.

Table 7.1: Calculation of entering water for the Bjørnefjorden Bridge

Volumes and element masses		
Case	Volume	Mass
	m^3	kg
1	275.0	281641
2	586.74	600821
3	231.75	237312

It is observed that the most critical scenario corresponds to case 2, in which the collision occurs with a direction of 45°. The masses shown in the table should were added to the USFOS model.

The entering water volume was calculated to investigate its effects on the response of the bridge; therefore, the effect was simulated as vertical forces and moments due to the eccentricity of the flooded compartments.

The load cases are presented in relation to the damaged compartments in fig. 7.2.

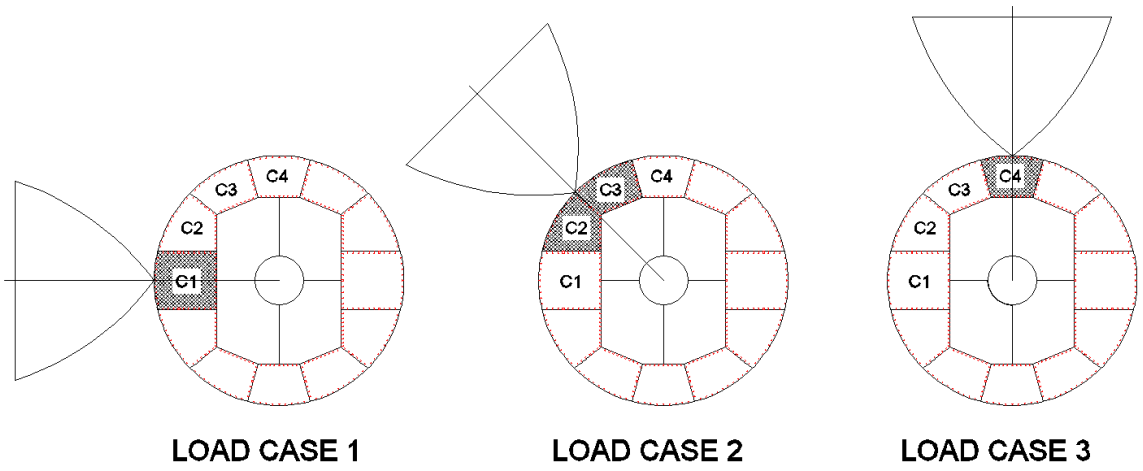

Figure 7.2: Collision load cases

The following table shows the forces associated with each load case. The moments have been calculated based on the eccentricities form the center of the cross section.

Table 7.2: Plates thickness of the original and redesigned models

Load cases forces due to flooding of the compartments						
Load Case	Mass	Force	$\bar{X}$	$\bar{Y}$	Mx	My
	kg	MN	m	m	MNm	MNm
1	281641	2.76	11.18	0.00	30.9	0.00
2	600821	5.90	8.5469	8.5152	50.2	50.4
3	237312	2.33	0.00	12.593	0.00	29.4

7.2.1 Comparison of the load cases due to flooding of compartments

The forces and moments resulting from the analysis were applied in the USFOS model and the displacements of the control nodes were compared considering the 3 load cases.

Table 7.3: Maximum node displacements considering static flooded conditions

Maximum node displacements (m)				
Node	Original	Case 1	Case 2	Case 3
13174	0.842	0.858	0.832	0.844
11174	0.828	0.845	0.818	0.831
11211	1.077	1.109	1.082	1.083
13246	0.770	0.820	0.737	0.778
11246	0.756	0.801	0.725	0.764
1013069	0.753	0.798	0.723	0.761

According to the results, the variation of the displacements was not considered relevant to endanger the structure. The acceleration of the node 11246 was compared. Fig. 7.5 compares the variation of the acceleration considering the flooded conditions and the original model.

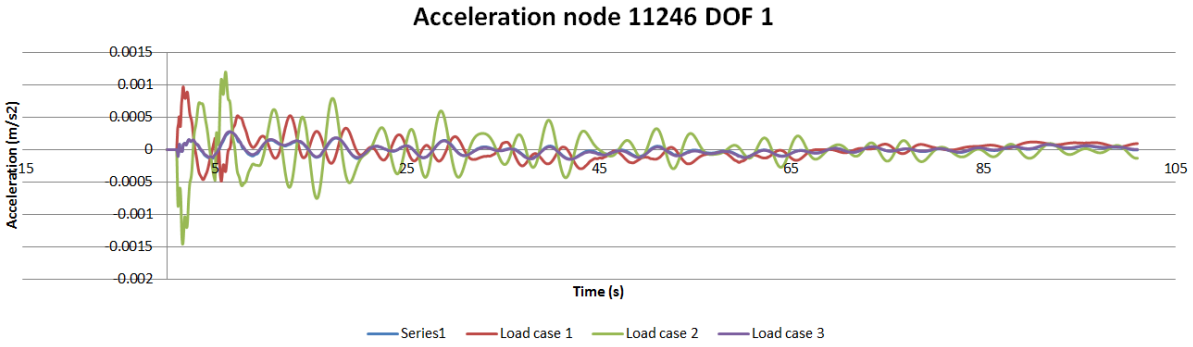

Figure 7.3: Acceleration comparison node 11246 DOF1

The acceleration of all the control nodes was investigated under the three conditions and later compared in terms of the original configuration. All the control nodes reached the maximum accelerations under the load condition 2.

7.3 Failure in the form of fracture of tethers

The effects due to fracture of tethers was investigated in the form of artificial fracture of the tethers has been conducted.

Fig. 7.4 presents a lower view of the floating structures in order to identify the tethers.

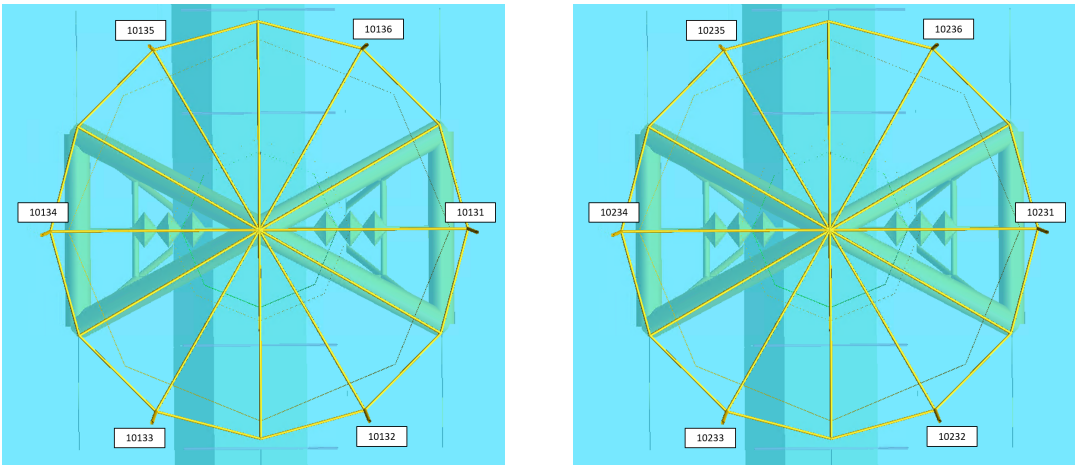

Figure 7.4: Bottom view of the tethers for identification

The failure in the form of fracture of tethers was simulated by applying a increasing axial force to the tethers. Later the stresses and forces are compared for different scenarios.

7.3.1 Case for analysis

One scenario for the fracture was simulated for tether 10134. The scenario considers an increasing tension load.

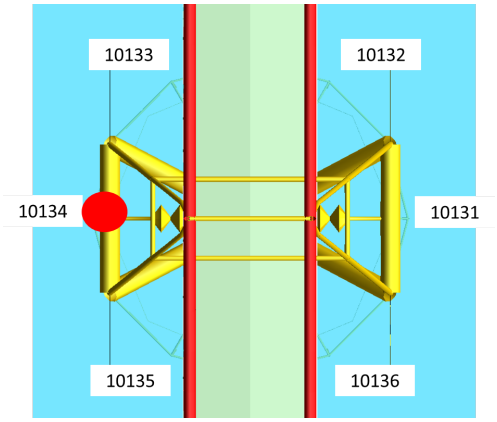

Figure 7.5: Selection of tether for failure simulation

7.3.2 Stress-level in critical components and description

An axial load was applied to the tether 10134 to increase the plastic utilization. Under this scenario, the force in the other tethers varied dramatically. Fig. 7.6 presents the force variation of the tethers. The left side is associated to the failed pylon, while the right side is associated to the undisturbed pylon.

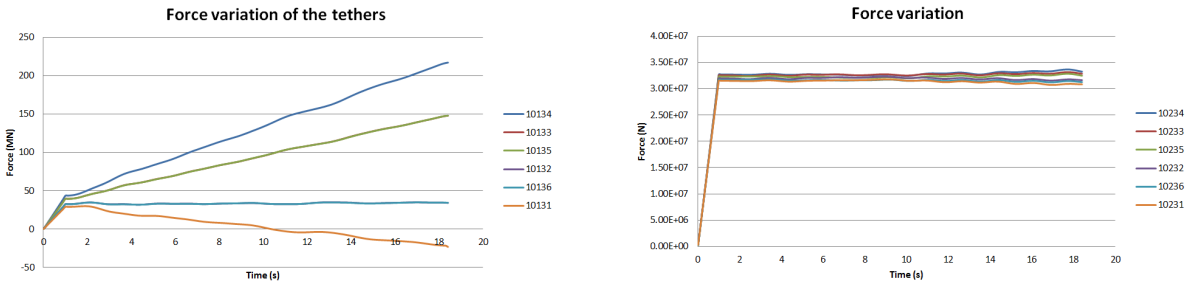

Figure 7.6: Variation of the element forces for the failure case 1

Fig. 7.9 indicates the response under this scenario. The tethers of the failed pylon reached high plastic utilization factors, while the tethers from the undisturbed pylon remained stable. .

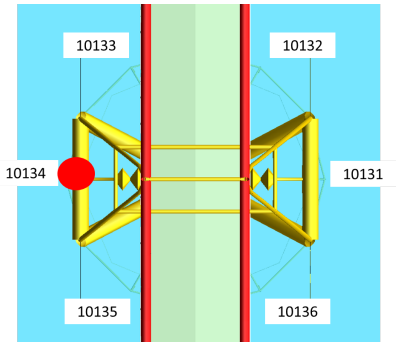

Figure 7.7: Failure of tether

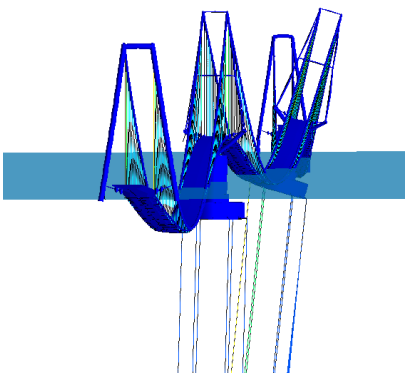

Figure 7.8: Plastic utilization

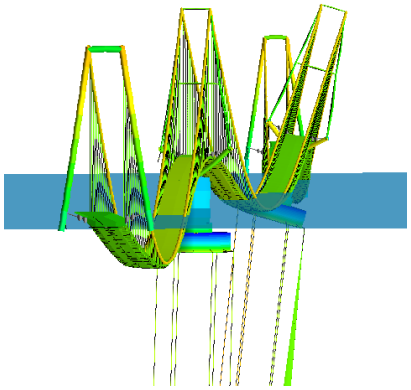

Figure 7.9: Element force

Several combinations might be taken into account, for example applying a lateral load or combining design environmental loads. This calculations might be included for future work.

Chapter 8

Discussions

Some of the main observations throughout this work in relation to modeling considerations, complexities in the modeling process and results are discussed.

8.1 Modeling considerations

To decrease the computation time, the LS-DYNA model is reduced to half of the pylon. For different collision directions, the pylon was rotated to run the simulations. The edges of the pylon were fixed in the six degrees of freedom.

In order to obtain a representative results in LS-DYNA, a constant speed of 10 m/s was applied to the ship during the collision; furthermore all the results are related to this velocity. On the other hand when running the simulations in USFOS, the velocity was set to 11.3 m/s. This difference was not considered significant for the calculations.

When defining the contact conditions, both the dynamic and static friction coefficients were set to 0.3 for the automatic surface to surface, but the automatic single surface condition considered a value of 0.35. These values were suggested by the supervision.

The most likely collision scenario is assumed perpendicular to the bridge, the second most likely case is when the collision occurs with an angle of 45 degrees and the least likely scenario is assumed parallel to the bridge, thus the case deeply studied was the first one.

The collision simulations in USFOS considered a simple and a double spring system. Hyperelastic springs are used in order to bounce the ship back, non linear springs ares used to repre-

sent the force-deformation curves from LS-DYNA.

8.2 Modelling Complexities

The mesh creation for the finite element model was oh high complexity because the continuity for all the structures must be ensured. Therefore the difficulty of the meshing is in function of the geometry of the model.

The simulations in LS-DYNA required 40 hours of computations to simulate and average time of 0.9 s. This is a considerable limitation because the model was improved by iterations. The initial simulations were computed along 12 hours; however the results were not descriptive enough to investigate the collision mechanism.

The input for the hourglass control was obtained by iterations and considering previous recommendations form the supervisor. For initial computations, the hourglass energy reached considerable negative values, thus new input was tested.

The simulations in USFOS were sensitive to the force deformation curves. When very close points of the curve are included, the simulations stopped indicating errors. Curves with initial positive slopes were be provided to avoid computation errors.

Refined time steps were provided to USFOS in order to run the simulations. Very large time steps might lead to errors in the simulations, this might be associated to the used time step method.

Conducting simulations in USFOS required knowledge on scripting, the user is required to modify the model by modifying the scripts and using specific commands.

8.3 LS-DYNA and USFOS results

According to the design, considerable deformations are expected for the ship during the collision. The energy dissipation for strength is considered under the strength design zone. Furthermore the pylon is assumed strong to counteract the collision.

Considerable displacements for the bridge are expected under a ship collision scenario. Maximum lateral displacements of about 15 m were computed. When comparing the displace-

ments of the models with one and two spring systems, the differences were not significant. So, both models were considered representative.

When simulating the flooded compartments, the maximum displacements and forces changed slightly, however a final revision suggested a low level of accuracy for this calculation. Future simulations might be improved.

For most of the cases, detailed discussions are included directly with the results.

Chapter 9

Conclusions and recommendations for further work

The structural design of the pylon was achieved by a long iterative process after several collision simulations and the analysis of the structural response. Later, the thickness and material properties were input in order to provide sufficient strength to reinforce the structure.

When programming the collision simulations, the computation time is a mandatory aspect to take into account in order to schedule an effective logistic program. The initial simulations took about 12 to 14 hours to be completed and the simulated time was about 0.3 s. On the other hand, the final LS-DYNA simulations considered a computation time of 40 hours and the simulated time was about 0.89 s.

The most feasible scenario considers a ship colliding perpendicularly to the longitudinal center line of the bridge. However the worst scenario in terms of the flooded condition corresponds to the load case 2 with a collision direction of 45 °. According to the results, the maximum displacements and accelerations present under this load cases.

No significant changes were identified when comparing the resultant force of the same model in terms of different collision directions. On the other hand, when comparing the resultant force for the original and the reinforced models, considerable fluctuation were identified as a result of a modified interaction between the pylon and the ship.

For future work, it is recommended to use more ships as an ice-strengthened ro-ro vessel in order to improve the validity of the design. At the same time, the draft variation might suggest

new modifications.

Even when the pylon is not penetrated for the final design, considerable thickness reduction presents for the outer plate. This suggest the need to repair and reinforce the pylon after collision.

Contemplating three stiffening rings is considered the best option for the design. One ring did not provide enough stiffness to avoid considerable damage. Furthermore the recommendation is to provide 3 stiffening rings. NV A36 steel is considered a suitable option for the design with an intermediate cost level.

For the initial LS-DYNA simulations, the bulb penetrated the outer plate of the pylon immediately after contact. This was the main argument to implement changes to strengthen the pylon. As a conclusion ,the final design was considered highly resistant against ship collision. The design was guided by building up a structure capable to minimize the damage of the pylon in order to decrease the possibility of flooding and collapse.

As a conclusion, the pylon is considered highly rigid to overcome the ship collision. Based on the comparison of the final design and the simulation against a rigid wall, the pylon performs under the strength design zone of the energy dissipation curve.

When implementing the force-deformation curve in USFOS, the maximum displacement of the bridge girder at the tower was 15.232; while the displacement at the top of the tower was 15.515. Thus the pylon is expected to behave as a rigid body with stable lateral motions as a result of the tethers and the whole structural stiffness.

When running the LS-DYNA simulations, the definitions of the contact and boundary conditions play a significant role in obtaining accurate results. A special investigation must be considered when defining the hourglass, because the energy results are dramatically sensible to the selected value.

Considerable variation of forces were identified during the simulation of the fracture of one tether. As a conclusion, the tethers must redistribute the forces to reach equilibrium; when loosing one tether, the tower may present rotations which should be verified for future work.

List of Figures

List of Tables

Appendix A

Acronyms

FTA Fault tree analysis

MTTF Mean time to failure

RAMS Reliability, availability, maintainability, and safety

DOF Degree of freedom

NPRA The Norwegian Public Roads Administration

NTP National Transport Plan

TLP Tension leg platform

JNTO Japan National Tourism Organization

CHRE39 Coastal Highway Route E39

FEM Finite Element Method

LLNL Lawrence Livermore National Laboratory

DNV-GL Norske Veritas and Germanischer Lloyd: DNV-GL

ABS The American Bureau of Shipping

ALC The Accidental Limit States

APPENDIX 1: Initial proposals for the structural arrangement considering different number of bulkheads.

4 BULKHEADS

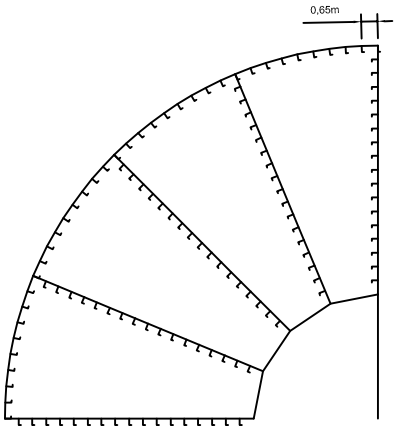

1 BULKHEADS

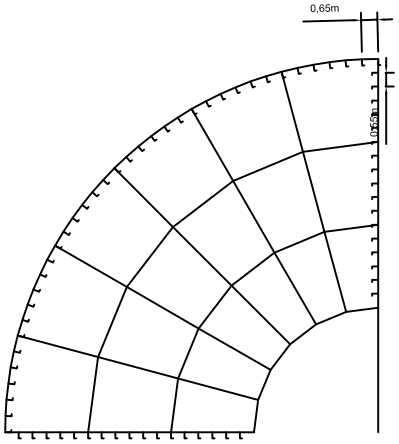

5 BULKHEADS

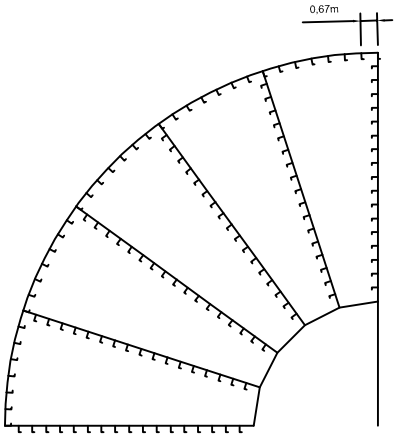

2 BULKHEADS

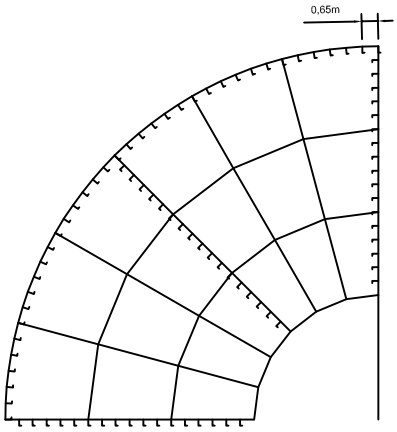

6 BULKHEADS

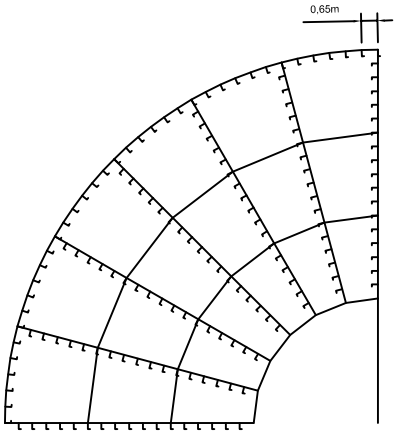

3 BULKHEADS

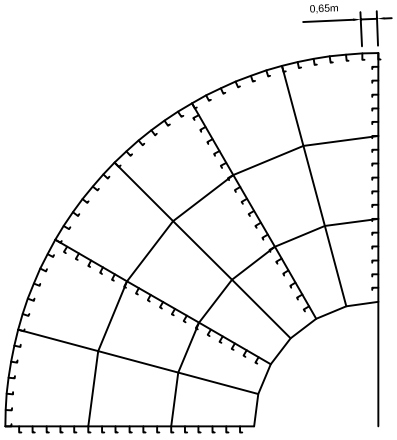

Appendix 2. Proposals for structural arrangements of the decks

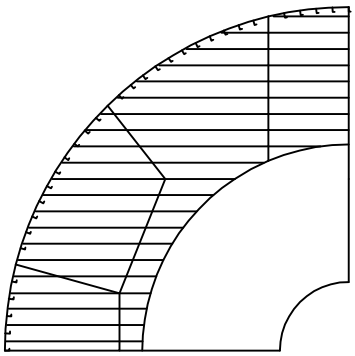

Configuration 1

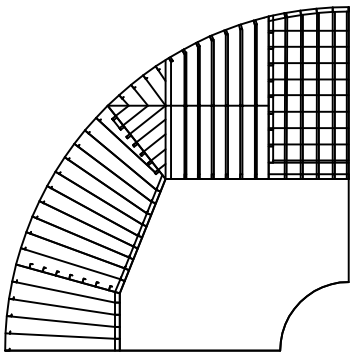

Configuration 2

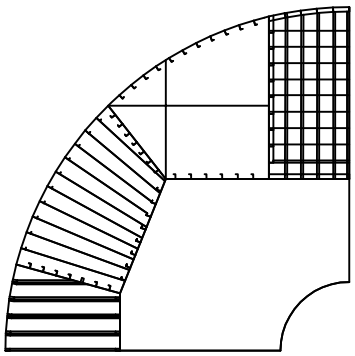

Configuration 3

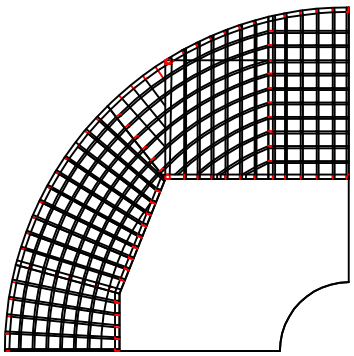

Configuration 4

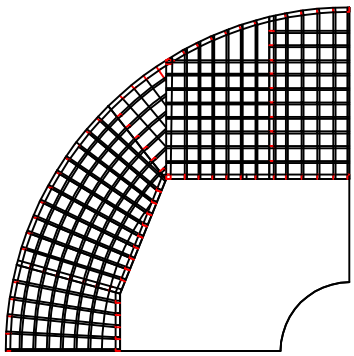

Configuration 5

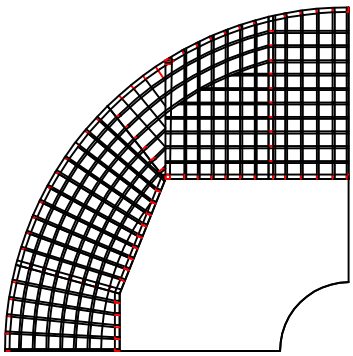

Configuration 6

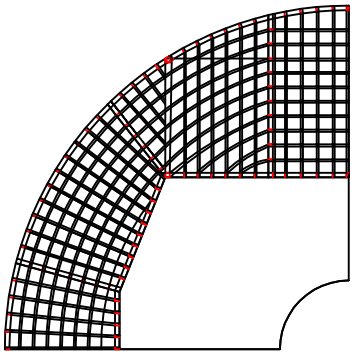

Configuracion 7

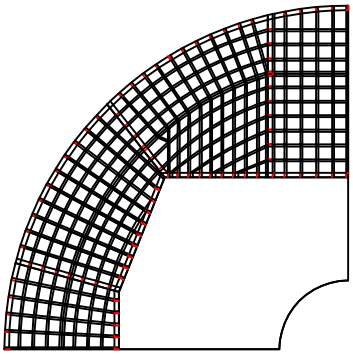

Final configuration

T203x37.3 Page 79
HSS 203x9.5 Page 103
I305x59.8 Page bf=203mm
I610x158 Pag 53 bf=200 D=622

APPENDIX 3. CONTOUR LS-DYNA RESULTS FOR THE SHIP COLLISION WITH THE DESIGN PYLON

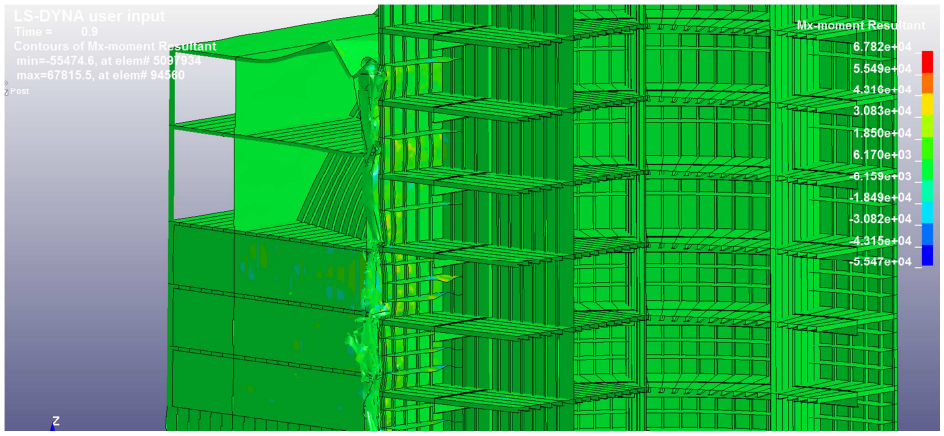

Contours of Mx-moment Resultant

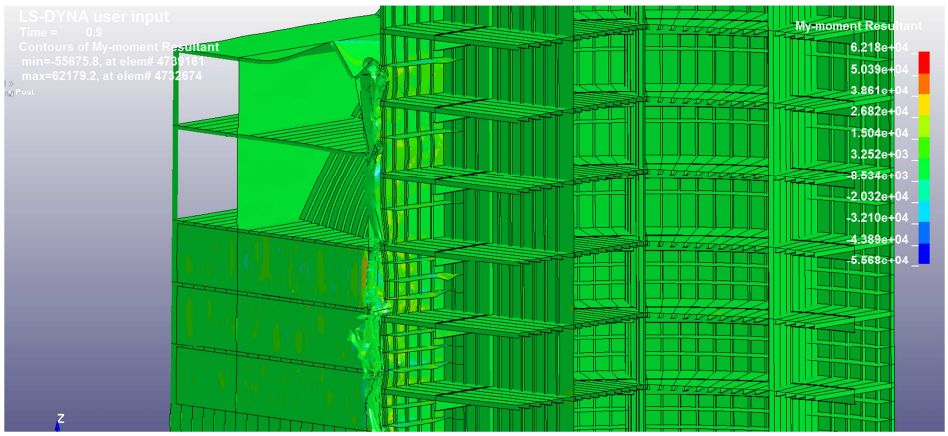

Contours of My-moment Resultant

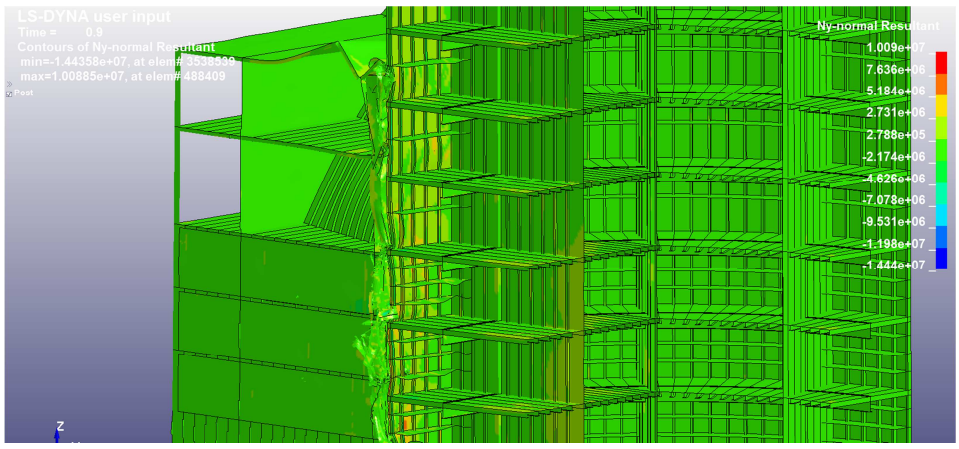

Contours of Ny-normal Resultant

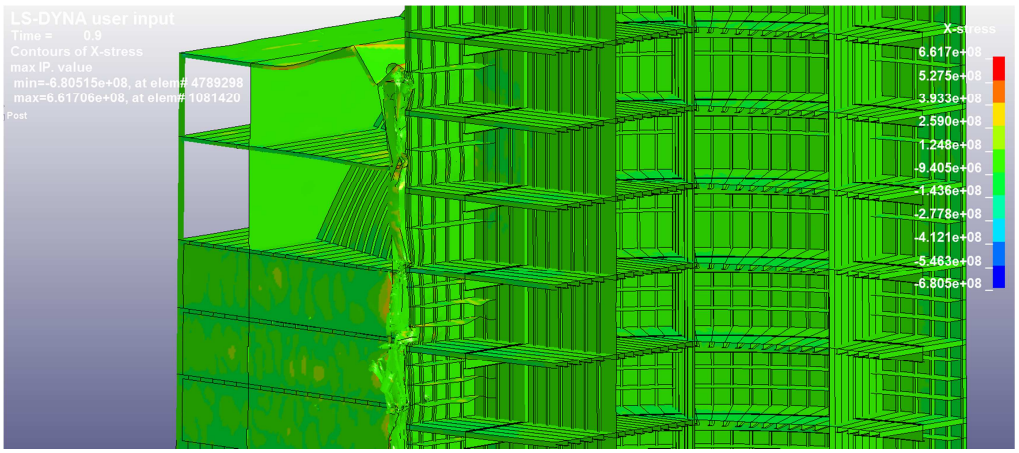

Contours of X-stress

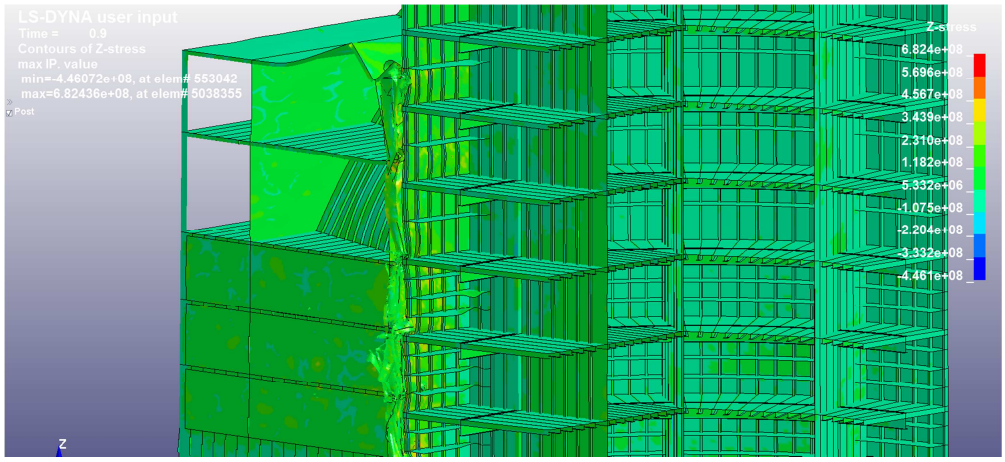

Contours of Z-stress

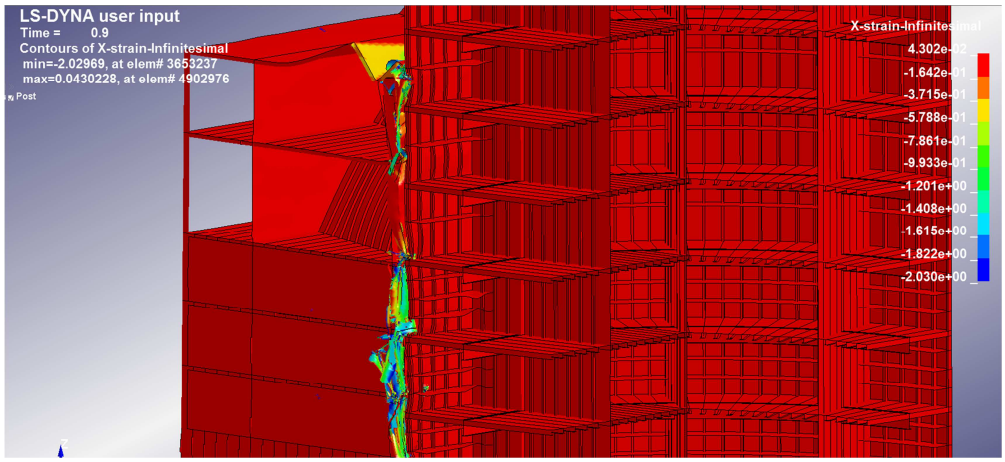

Contours of X-strain-Infinitesimal

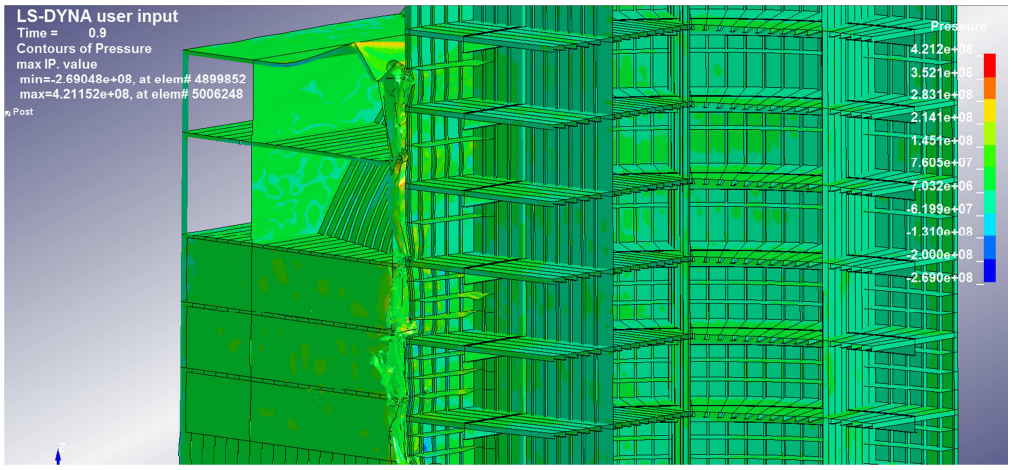

Contours of Pressure

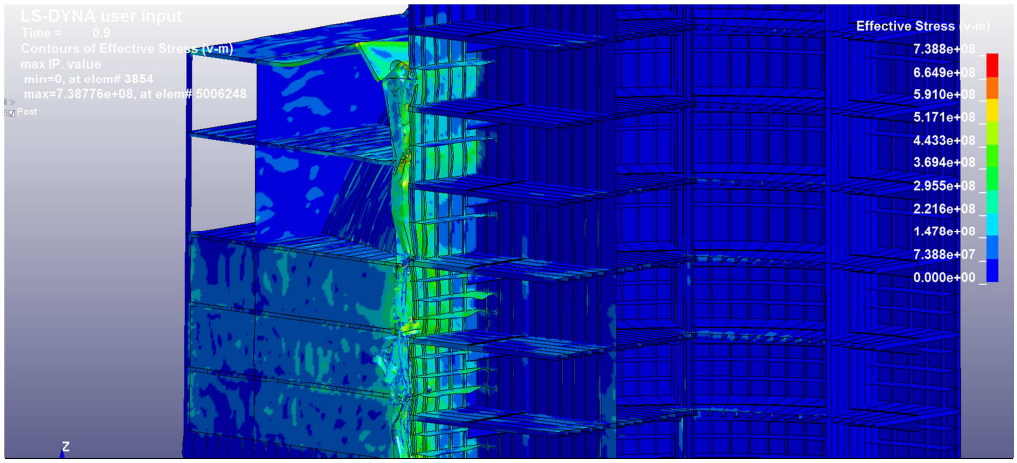

Contours of Effective Stress (V-m)

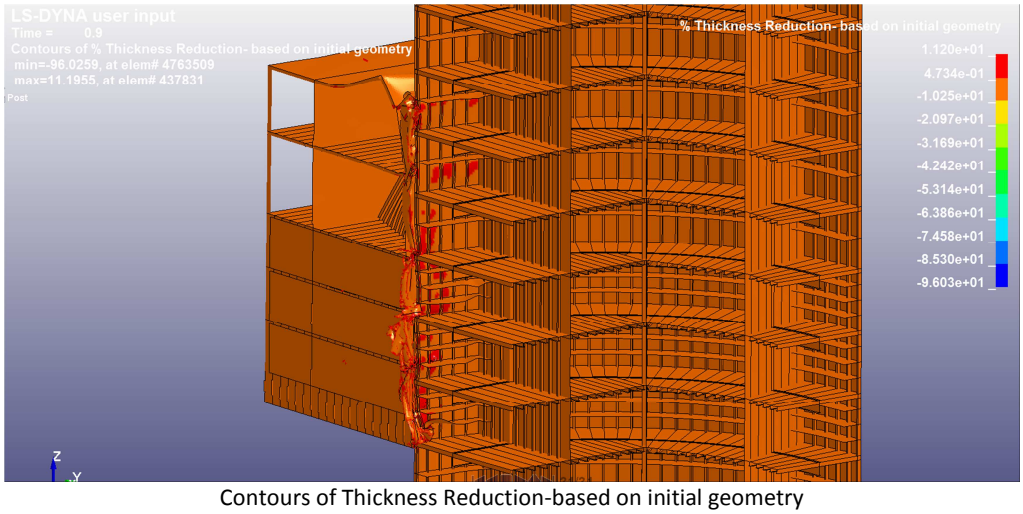

Contours of Thickness Reduction-based on initial geometry

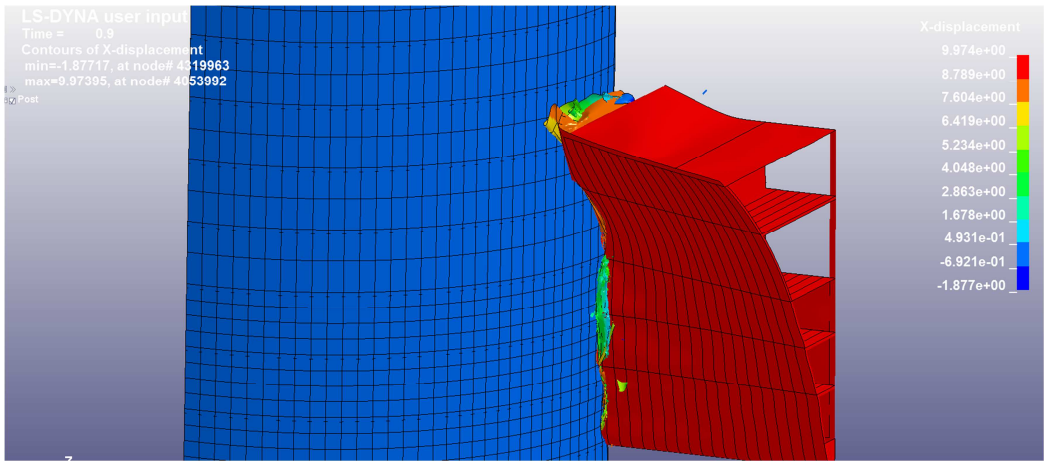

Contours of X-displacement

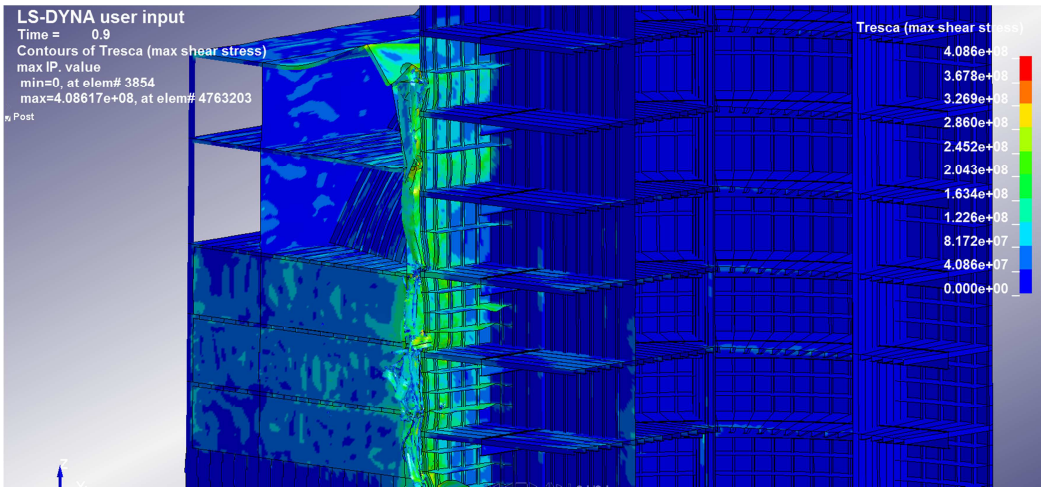

Contours of Tresca (max shear stress)

Bibliography

Akashi Suspension Bridge, WikiArquitectura. https://en.wikiarquitectura.com/building/akashi-kaikyo-bridge/. Accessed: 2017-06-10.

Bjørnafjorden Norway, Google Maps. https://www.google.com/#q=google+maps. Accessed: 2017-06-10.

Ferjefri E39, Statens Vegvesen. http://www.vegvesen.no/vegprosjekter/ferjefriE39. Accessed: 2017-06-10.

Into Japan: The Official Guide,Japan National Tourism Organization. https://www.jnto.go.jp/eng/spot/bridges/akashi-kaikyo-bridge.html. Accessed: 2017-06-10.

LSTC website, LSTC. http://www.lstc.com/products/ls-dyna. Accessed: 2017-06-10.

Nordhordland Bridge, BridgeInfo. https://www.bridgeinfo.net/bridge/index.php?ID=43. Accessed: 2017-06-10.

Nordhordland Bridge, Wikipedia The Free Encyclopedia. https://en.wikipedia.org/wiki/Nordhordland_Bridge. Accessed: 2017-06-10.

American Bureau of Shipping (2013). *Accidental load analysis and design for offshore structures.* American Bureau of Shipping, Texas, United States of America.

DNV-GL (2010). *Recommended Practice DNV-RP-C204, Design against accidental loads.* Det Norske Veritas and Germanischer Lloyd.

Erik Frydenlund, Kaare Flaate, Håvard Østlid (2005). *Strait Crossings 2013.* Statens vegvesen, Bergen, Norway.

Gudmestad, O. T. (2013). *Strait Crossings 2013-Proceedings Design basis for strait crossings*. Statens Vegvesens, Bergen, Norway.

Harald O. (2016). *Analysis and Design of Bjørnafjorden TLP Supported Suspension Bridge Subjected to Large Ship Collisions and Extreme Environmental Loads*. Norwegian University of Science and Technology, Trondheim, Norway.

Jacob Fish (2007). *A First Course in Finite Elements*. JohnWiley and Sons, Ltd, West Sussex, England.

Jakobsen, B. (2013). *Strait Crossings 2013 - Ship impacts on the floating pontoons supporting a multiple span suspension bridge*. Statens Vegvesens, Bergen, Norway.

John O. Hallquist (2006). *LS-DYNA Theory Manual*. Livermore Software Technology Corporation, California, United States of America.

Jørgen Amdahl (1988). *USFOS Theory Manual*. SINTEF, Trondheim, Norway.

Jørgen Amdahl (2001). *Nonlinear Analysis of Offshore Structures*. Research studies press LTD, Baldock Herdfordshire, England.

Jørgen Amdahl (2017). *Graphic provided information*. Trondheim, Norway.

LSTC (2006). *LS-DYNA Keyword user´s manual - Volume 1*. Livermore Software Technology Corporation, California, United States of America.

Mr. Olav Ellevset, (2014). *Norwegian Coastal Highway Route E39 - Status Overview*. Statens vegve, Oslo, Norway.

Romero V. (2016). *Analysis and Design of Bjørnafjorden TLP Supported Suspension Bridge Subjected to Large Ship Collisions and Extreme Environmental Loads*. Norwegian University of Science and Technology, Trondheim, Norway.

Skorpa, L. (2013). *Strait Crossings 2013 - Crossing the deep and wide fjords on the Western coast of Norway with fixed connections*. Statens Vegvesens, Bergen, Norway.

Yanyan Sha (2017). *Multi-span suspension bridge on floating foundations - behaviour under ship impact.* Norwegian University of Science and Technology, Vancouver, Canadae.

Yun Lee (2013). *Strait Crossings 2013 - Impact Analysis of submerged floating tunnel for conceptial design.* Institute of Ocean Science and Technology, Gyeonggi, South Korea.